Generalized Parton Distributions

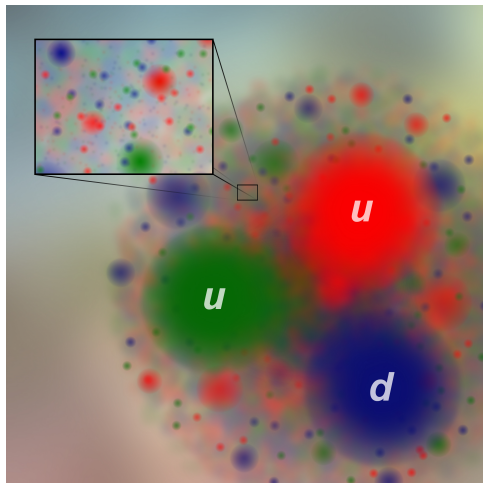

Jakub Wagner

Theoretical Physics Department
National Center for Nuclear Research

EIC PL Seminar, 26th April 2021

work in collaboration with:
L. Szymanowski (NCBJ), P. Sznajder (NCBJ), O. Grocholski (NCBJ & UW)
B. Pire (Ecole Polytechnique), H. Moutarde (CEA), J.-P. Lansberg (IJCLab - Paris Saclay U.)

Deep Inelastic Scattering $e\,p \to e\,X$

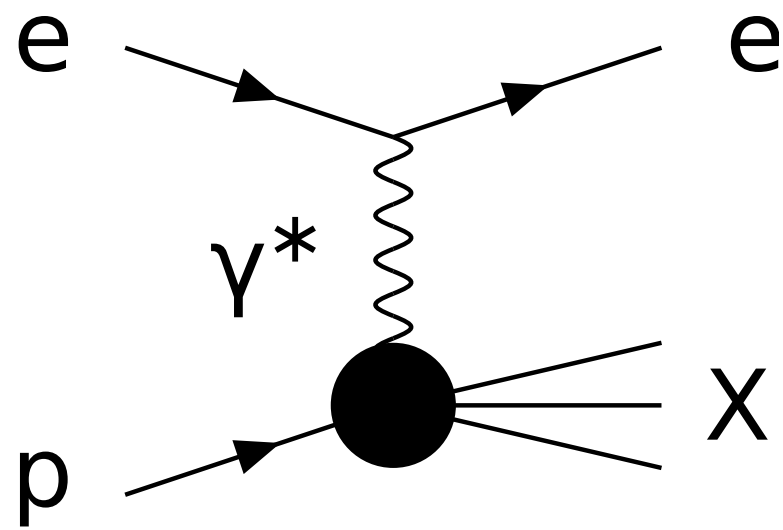

In the Björken limit i.e. when the photon virtality $Q^2 = -q^2$ and the squared hadronic c.m. energy $(p+q)^2$ become large, with the ratio $x_B = \frac{Q^2}{2p\cdot q}$ fixed, the cross section factorizes into a hard partonic subprocess calculable in the pertutbation theory, and a parton distributions.

DIS

- Parton distributions encode the distribution of longitudinal momentum and polarization carried by quarks, antiquarks and gluons within fast moving hadron
- PDFs don't provide infomation about how partons are distributed in the transverse plane and ...
- about how important is the orbital angular momentum in making up the total spin of the nucleon.
- For the last 20 years - growing interest in the exclusive scattering processes, which may shed some light on these issues through the generalized parton distributions (GPD).

DVCS

The simplest and best known process is Deeply Virtual Compton Scattering: $e\,p \to e\,p\,\gamma$

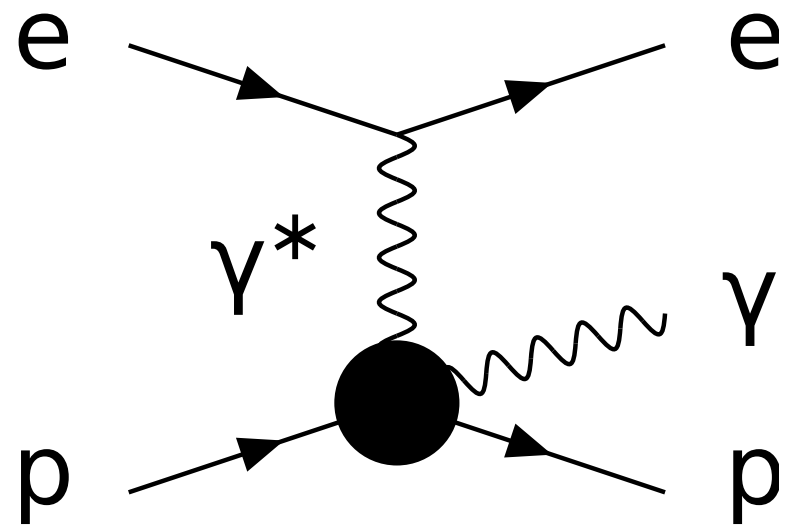

Factorization into GPDs and perturbative coefficient function - on the level of amplitude.

$$\begin{aligned} \text{DIS}: &\qquad \sigma = \text{PDF} \otimes \text{partonic cross section} \\ \text{DVCS}: &\qquad \mathcal{M} = \text{GPD} \otimes \text{partonic amplitude} \end{aligned}$$

DVCS

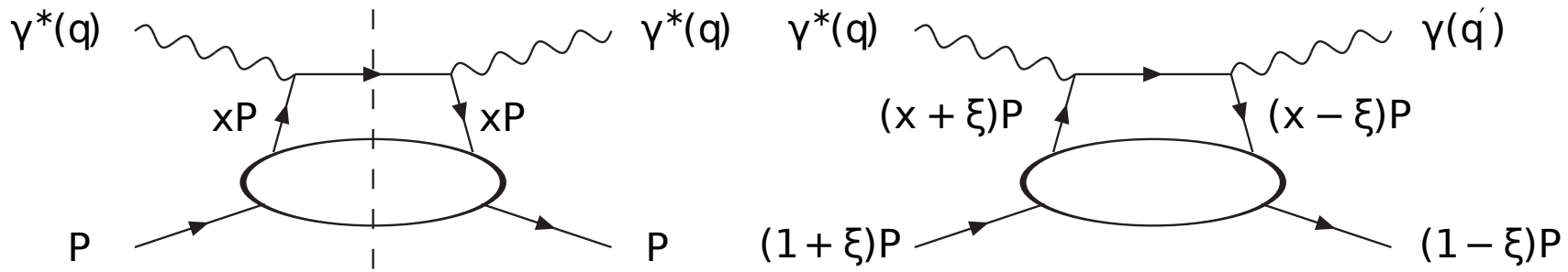

Figure: Deep Inelastic Scattering cross section is given by the imaginary part of diagram (a). Amplitude of Deeply Virtual Compton Scattering is given by diagram (b).

Symmetric variables

$$P = \frac{p + p'}{2} \quad , \quad \bar{q} = \frac{q + q'}{2}$$

Generalized Bjorken variable:

$$\xi = \frac{-\bar{q}^2}{2\bar{q} \cdot P} \approx \frac{x_B}{2 - x_B} \quad , \quad x_B = \frac{Q^2}{2q \cdot p}$$

momentum transfer between proton initial and final state:

$$t = (p' - p)^2$$

In the convenient reference frame, where P has only positive time- and z-components, and light vector are defined as:

$$v_+ = (1, 0, 0, 1)\frac{1}{\sqrt{2}} \quad , \quad v_- = (1, 0, 0, -1)\frac{1}{\sqrt{2}}$$

(-2ξ) has an interpretation of the fraction of momentum transport in "+" direction.

GPD definition.

$$
\begin{aligned}
F^q &= \frac{1}{2}\int \frac{dz^-}{2\pi}\, e^{ixP^+z^-} \langle p'|\, \bar{q}(-\frac{1}{2}z)\, \gamma^+ q(\frac{1}{2}z)\, |p\rangle \Big|_{z^+=0,\,\mathbf{z}=0} \\
&= \frac{1}{2P^+}\left[H^q(x,\xi,t)\, \bar{u}(p')\gamma^+ u(p) + E^q(x,\xi,t)\, \bar{u}(p')\frac{i\sigma^{+\alpha}\Delta_\alpha}{2m} u(p) \right], \\
F^g &= \frac{1}{P^+}\int \frac{dz^-}{2\pi}\, e^{ixP^+z^-} \langle p'|\, G^{+\mu}(-\frac{1}{2}z)\, G_\mu{}^+(\frac{1}{2}z)\ |p\rangle \Big|_{z^+=0,\,\mathbf{z}=0} \\
&= \frac{1}{2P^+}\left[H^g(x,\xi,t)\, \bar{u}(p')\gamma^+ u(p) + E^g(x,\xi,t)\, \bar{u}(p')\frac{i\sigma^{+\alpha}\Delta_\alpha}{2m} u(p) \right],
\end{aligned}
$$

- interpretation, ERBL, DGLAP

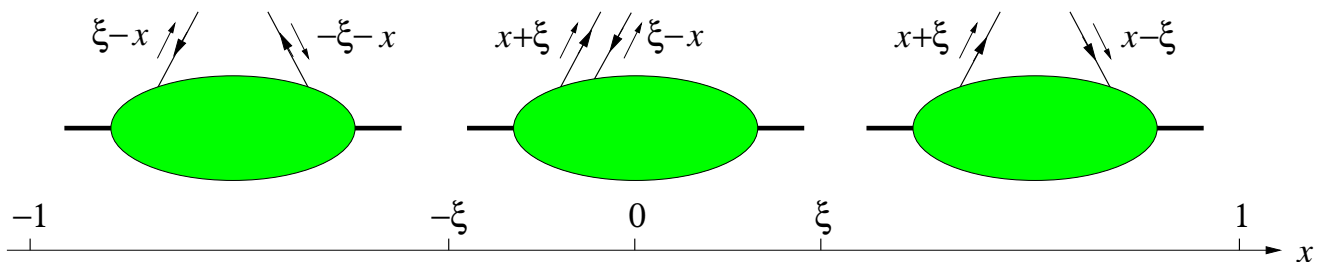

- Factorization scale dependance,
- Three variables x, ξ, t .

GPD - properties

- Forward limit:

$$\begin{aligned} H^q(x,0,0) &= q(x)\,, \qquad \text{for} \qquad x>0\,, \\ H^q(x,0,0) &= -\bar{q}(x)\,, \qquad \text{for} \qquad x<0\,, \\ H^g(x,0,0) &= xg(x)\,, \end{aligned}$$

  similarly for polarized disributions and PDFs.

- Reduction to form factors:

$$\int_{-1}^{1} dx\, H^q(x,\xi,t) = F_1^q(t), \qquad \int_{-1}^{1} dx\, E^q(x,\xi,t) = F_2^q(t),$$

  where the Dirac and Pauli form factors

$$\langle p'|\,\bar{q}(0)\gamma^\mu q(0)\,|p\rangle = \bar{u}(p')\left[\,F_1^q(t)\,\gamma^\mu + F_2^q(t)\,\frac{i\sigma^{\mu\alpha}\Delta_\alpha}{2m}\,\right]u(p),$$

- polynomiality and positivity

GPD - properties

- Ji sum rule:

$$\lim_{t\to 0}\int_{-1}^{1} dx\; x\left[H_f(x,\xi,t)+E_f(x,\xi,t)\right]=2J_f$$

where J_f is fraction of the proton spin carried by quark f (including spin and orbital angular momentum).

connection with energy-momentum tensor, more in Paweł Sznajder talk in 2 weeks

- Impact parameter representation, at $\xi=0 \quad \Rightarrow \quad -t=\Delta_\perp^2$:

$$H(x,\mathbf{b}_\perp)=\int \frac{d^2\boldsymbol{\Delta}_\perp}{(2\pi)^2} e^{-i\mathbf{b}_\perp\cdot\boldsymbol{\Delta}_\perp} H(x,0,-\boldsymbol{\Delta}_\perp)$$

can be interpreted as probability of finding a parton with longitudinal momentum fraction x at a given $\mathbf{b}_\perp$.

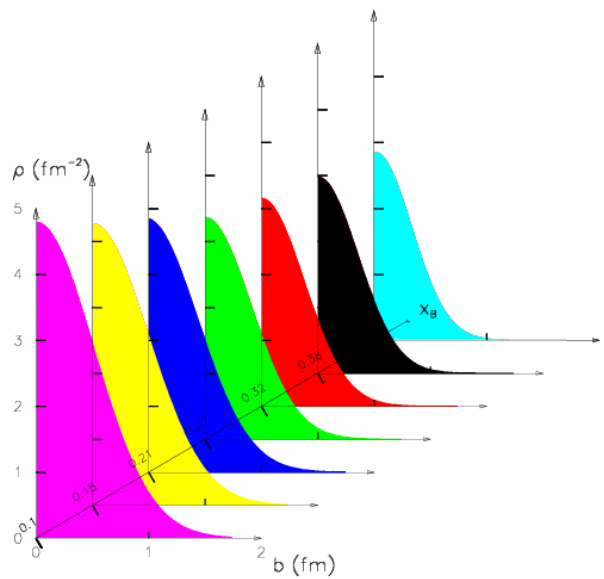

H. Moutarde, P. Sznajder, J. Wagner, Eur.Phys.J. C78 (2018)

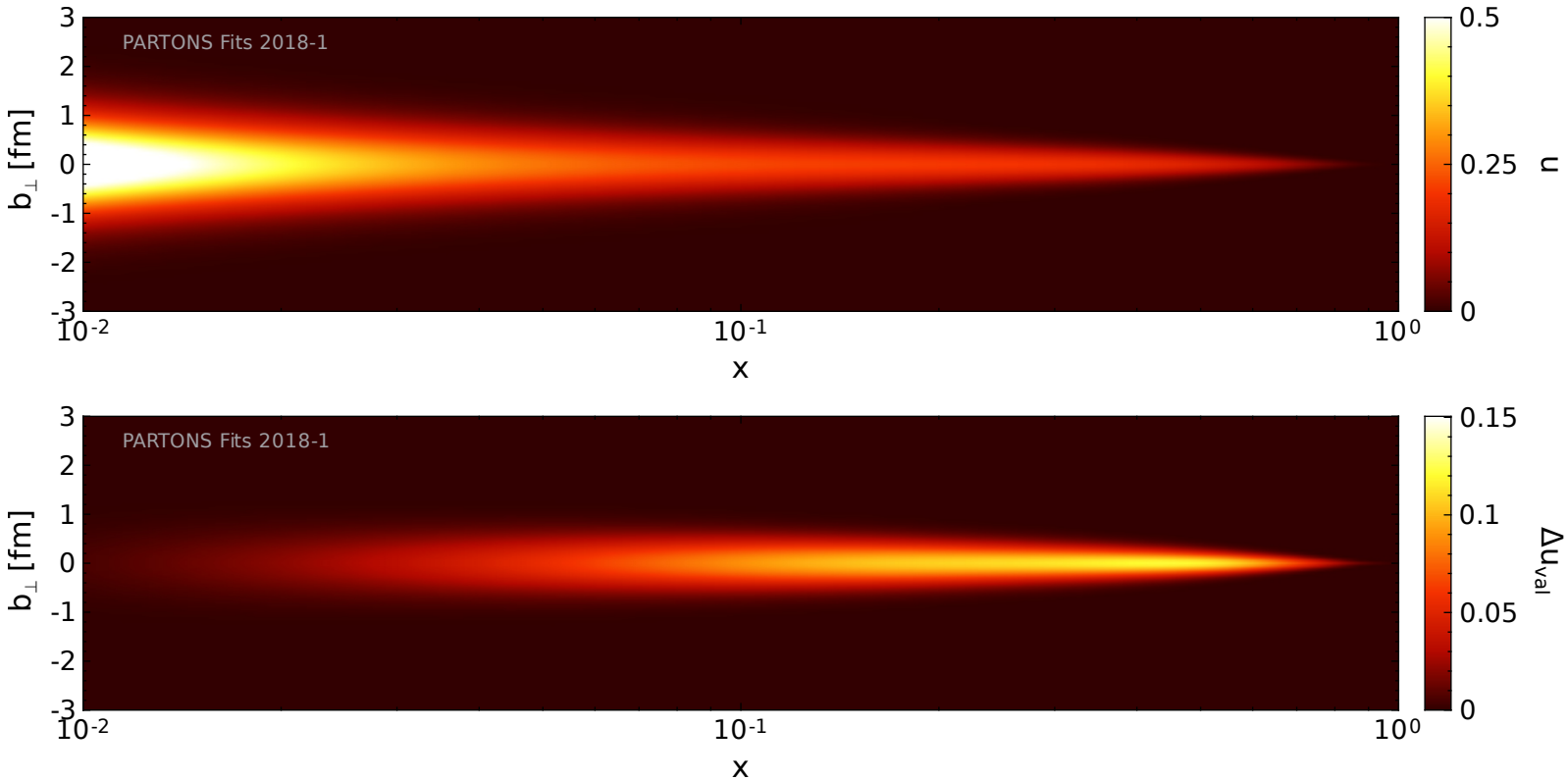

Figure: Position of up quarks in an unpolarized proton (upper plot) and longitudinal polarization of those quarks in a longitudinally polarized proton (lower plot) as a function of the longitudinal momentum fraction x. For the lower plot only the valence contribution is shown.

GPDs

- GPDs enter factorization theorems for hard exlusive reactions (DVCS, deeply virtual meson production, TCS etc.), in a similar manner as PDFs enter factorization theorems for inclusive (DIS, etc.)
- GPDs are functions of x, t, ξ, μ_F^2
- First moment of GPDs enters the Ji's sum rule for the angular momentum carried by partons in the nucleon,
- 2+1 imaging of nucleon,
- Deeply Virtual Compton Scattering (DVCS) is a golden channel for GPDs extraction,

Reviews:
- Belitsky, Radyushkin, *Phys.Rept. 418*
- Diehl, *Phys.Rept. 388*
- Boffi, Pasquini, *Riv.Nuovo Cim. 30*
- Kumericki, Liuti, Moutarde, *Eur.Phys.J.A 52*

DVCS - variables

Four variables needed to describe $ep \longrightarrow ep\gamma$ at fixed beam energy. Usually : Q^2, x_B, t and ϕ:

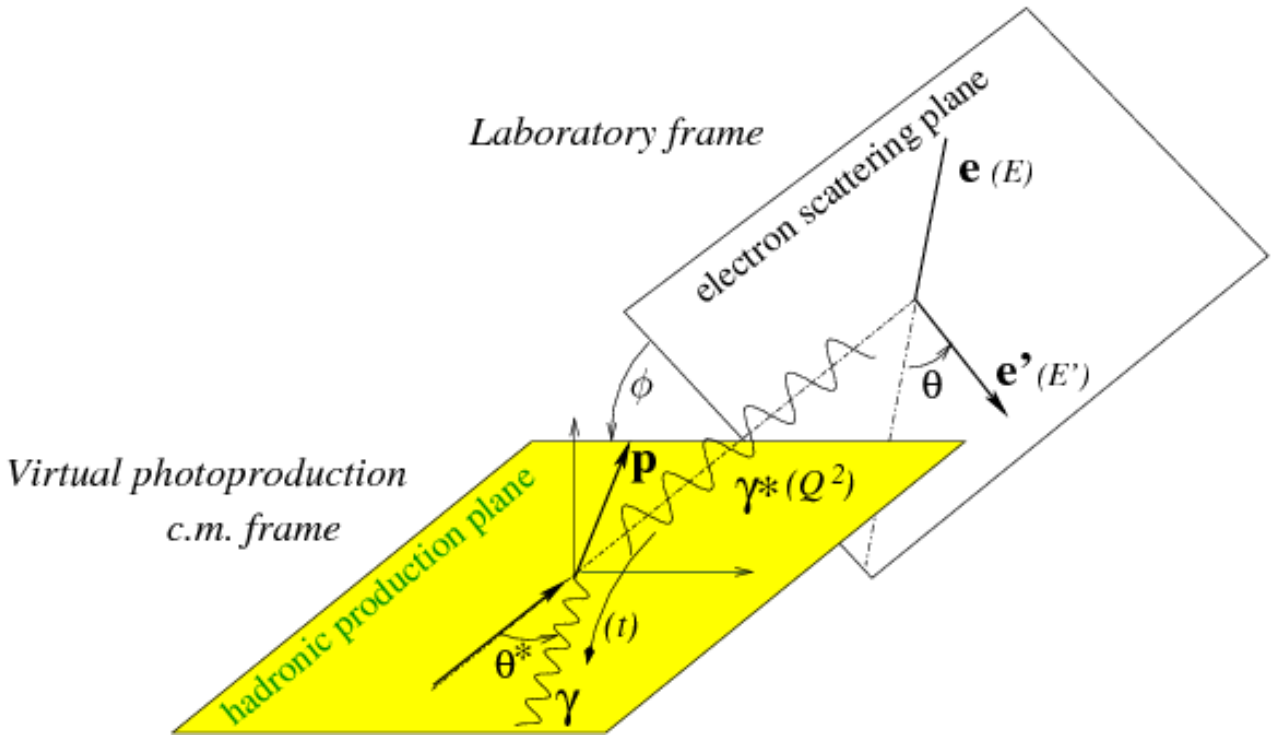

Coefficient functions and Compton Form Factors

CFFs are the GPD dependent quantities which enter the amplitudes. They are defined through relations:

$$\mathcal{A}^{\mu\nu}(\xi,t) = -e^2 \frac{1}{(P+P')^+}\,\bar{u}(P')\left[g_T^{\mu\nu}\left(\mathcal{H}(\xi,t)\,\gamma^+ + \mathcal{E}(\xi,t)\,\frac{i\sigma^{+\rho}\Delta_\rho}{2M}\right) + i\epsilon_T^{\mu\nu}\left(\widetilde{\mathcal{H}}(\xi,t)\,\gamma^+\gamma_5 + \widetilde{\mathcal{E}}(\xi,t)\,\frac{\Delta^+\gamma_5}{2M}\right)\right] u(P)\,,$$

,where:

$$\mathcal{H}(\xi,t) \quad = \quad + \int_{-1}^{1} dx \left(\sum_q T^q(x,\xi) H^q(x,\xi,t) + T^g(x,\xi) H^g(x,\xi,t) \right)$$

GPDs enter through convolutions! At LO in α_S:

$$^{DVCS}T^q = -e_q^2 \frac{1}{x+\xi-i\varepsilon} - (x \to -x)$$

$$^{DVCS}Re(\mathcal{H}) \sim P \int \frac{1}{x+\xi} H^q(x,\xi,t)\,, \qquad ^{DVCS}Im(\mathcal{H}) \sim i\pi H^q(\xi,\xi,t)$$

DVCS and BH

Figure 12 from Michel Guidal et al 2013 Rep. Prog. Phys. 76 066202

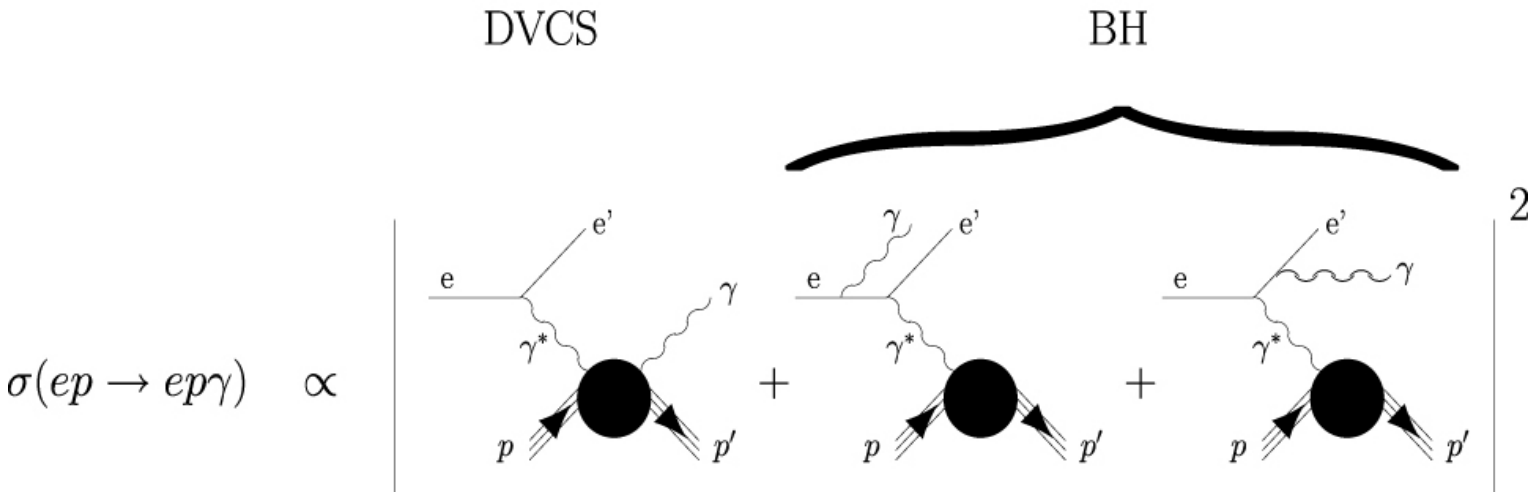

Observables

The $lp \to lp\gamma$ cross section on an unpolarized target for a given beam charge, e_l in units of the positron charge and beam helicity $h_l/2$ can be written as :

$$d\sigma^{h_l,e_l}(\phi) = d\sigma_{\rm UU}(\phi)\left[1 + h_l A_{\rm LU,DVCS}(\phi) + e_l h_l A_{\rm LU,I}(\phi) + e_l A_{\rm C}(\phi)\right] ,$$

If both longitudinally polarized positively and negatively charged beams are available (HERMES):

$$A_{\rm C}(\phi) = \frac{1}{4d\sigma_{\rm UU}(\phi)}\left[(d\sigma^{+}_{\rightarrow} + d\sigma^{+}_{\leftarrow}) - (d\sigma^{-}_{\rightarrow} + d\sigma^{-}_{\leftarrow})\right] .$$

$$\begin{aligned} A_{\rm LU,I}(\phi) &= \frac{1}{4d\sigma_{\rm UU}(\phi)}\left[(d\sigma^{+}_{\rightarrow} - d\sigma^{+}_{\leftarrow}) - (d\sigma^{-}_{\rightarrow} - d\sigma^{-}_{\leftarrow})\right] , \\ A_{\rm LU,DVCS}(\phi) &= \frac{1}{4d\sigma_{\rm UU}(\phi)}\left[(d\sigma^{+}_{\rightarrow} - d\sigma^{+}_{\leftarrow}) + (d\sigma^{-}_{\rightarrow} - d\sigma^{-}_{\leftarrow})\right] . \end{aligned}$$

If an experiment only has access to one value of e_l such as in Jefferson Lab, one can only measure the beam spin asymmetry $A_{\rm LU}^{e_l}$

$$A_{\rm LU}^{e_l}(\phi) = \frac{d\sigma^{e_l}_{\rightarrow} - d\sigma^{e_l}_{\leftarrow}}{d\sigma^{e_l}_{\rightarrow} + d\sigma^{e_l}_{\leftarrow}} ,$$

Observables

Target longitudinal spin asymmetry which reads :

$$A_{\mathrm{UL}}^{e_l}(\phi) = \frac{[d\sigma^{\overset{e_l}{\leftarrow\Rightarrow}} + d\sigma^{\overset{e_l}{\rightarrow\Rightarrow}}] - [d\sigma^{\overset{e_l}{\leftarrow\Leftarrow}} + d\sigma^{\overset{e_l}{\rightarrow\Leftarrow}}]}{[d\sigma^{\overset{e_l}{\leftarrow\Rightarrow}} + d\sigma^{\overset{e_l}{\rightarrow\Rightarrow}}] + [d\sigma^{\overset{e_l}{\leftarrow\Leftarrow}} + d\sigma^{\overset{e_l}{\rightarrow\Leftarrow}}]},$$

where the double arrows $\Leftarrow$ ($\Rightarrow$) refer to the target polarization state parallel (anti-parallel) to the beam momentum. The double longitudinal target spin asymmetry is defined in a similar fashion :

$$A_{\mathrm{LL}}^{e_l}(\phi) = \frac{[d\sigma^{\overset{e_l}{\rightarrow\Rightarrow}} + d\sigma^{\overset{e_l}{\leftarrow\Leftarrow}}] - [d\sigma^{\overset{e_l}{\leftarrow\Rightarrow}} + d\sigma^{\overset{e_l}{\rightarrow\Leftarrow}}]}{[d\sigma^{\overset{e_l}{\rightarrow\Rightarrow}} + d\sigma^{\overset{e_l}{\leftarrow\Leftarrow}}] + [d\sigma^{\overset{e_l}{\leftarrow\Rightarrow}} + d\sigma^{\overset{e_l}{\rightarrow\Leftarrow}}]},$$

The HERMES collaboration also had access to a transversally polarized target with both electrons and positrons:

$$A_{\mathrm{UT,I}}(\phi,\phi_S) = \frac{d\sigma^+(\phi,\phi_S) + d\sigma^+(\phi,\phi_S+\pi) - d\sigma^-(\phi,\phi_S) - d\sigma^-(\phi,\phi_S+\pi)}{d\sigma^+(\phi,\phi_S) - d\sigma^+(\phi,\phi_S+\pi) + d\sigma^-(\phi,\phi_S) - d\sigma^-(\phi,\phi_S+\pi)},$$

$$A_{\mathrm{UT,DVCS}}(\phi,\phi_S) = \frac{d\sigma^+(\phi,\phi_S) - d\sigma^+(\phi,\phi_S+\pi) - d\sigma^-(\phi,\phi_S) + d\sigma^-(\phi,\phi_S+\pi)}{d\sigma^+(\phi,\phi_S) - d\sigma^+(\phi,\phi_S+\pi) + d\sigma^-(\phi,\phi_S) - d\sigma^-(\phi,\phi_S+\pi)}.$$

Observables

$$
\begin{aligned}
A_C^{\cos\phi} &\propto \mathsf{Re}\left[F_1\mathcal{H} + \xi(F_1+F_2)\widetilde{\mathcal{H}} - \frac{t}{4m^2}F_2\mathcal{E}\right], \\
A_{LU,I}^{\sin\phi} &\propto \mathsf{Im}\left[F_1\mathcal{H} + \xi(F_1+F_2)\widetilde{\mathcal{H}} - \frac{t}{4m^2}F_2\mathcal{E}\right], \\
A_{UL,I}^{\sin\phi} &\propto \mathsf{Im}\left[\xi(F_1+F_2)(\mathcal{H}+\frac{\xi}{1+\xi}\mathcal{E}) + F_1\widetilde{\mathcal{H}} - \xi(\frac{\xi}{1+\xi}F_1 + \frac{t}{4M^2}F_2)\widetilde{\mathcal{E}}\right], \\
A_{LL,I}^{\cos\phi} &\propto \mathsf{Re}\left[\xi(F_1+F_2)(\mathcal{H}+\frac{\xi}{1+\xi}\mathcal{E}) + F_1\widetilde{\mathcal{H}} - \xi(\frac{\xi}{1+\xi}F_1 + \frac{t}{4M^2}F_2)\widetilde{\mathcal{E}}\right], \\
A_{LL,DVCS}^{\cos(0\phi)} &\propto \mathsf{Re}\Big[4(1-\xi^2)\big(\mathcal{H}\widetilde{\mathcal{H}}^* + \widetilde{\mathcal{H}}\mathcal{H}^*\big) - 4\xi^2\big(\mathcal{H}\widetilde{\mathcal{E}}^* + \widetilde{\mathcal{E}}\mathcal{H}^* + \widetilde{\mathcal{H}}\mathcal{E}^* + \mathcal{E}\widetilde{\mathcal{H}}^*\big) \\
&\qquad -4\xi\big(\frac{\xi^2}{1+\xi} + \frac{t}{4M^2}\big)\big(\mathcal{E}\widetilde{\mathcal{E}}^* + \widetilde{\mathcal{E}}\mathcal{E}^*\big)\Big], \\
A_{UT,DVCS}^{\sin(\phi-\phi_s)} &\propto \Big[\mathsf{Im}\left(\mathcal{H}\mathcal{E}^*\right) - \xi\mathsf{Im}\left(\widetilde{\mathcal{H}}\widetilde{\mathcal{E}}^*\right)\Big], \\
A_{UT,I}^{\sin(\phi-\phi_s)\cos\phi} &\propto \mathsf{Im}\Big[-\frac{t}{4M^2}\big(F_2\mathcal{H} - F_1\mathcal{E}\big) + \xi^2\big(F_1 + \frac{t}{4M^2}F_2\big)\big(\mathcal{H}+\mathcal{E}\big) \\
&\qquad -\xi^2\big(F_1+F_2\big)\big(\widetilde{\mathcal{H}} + \frac{t}{4M^2}\widetilde{\mathcal{E}}\big)\Big].
\end{aligned}
$$

World data on DVCS

H. Moutarde, P. Sznajder, J. Wagner, Eur.Phys.J. C79 (2019)

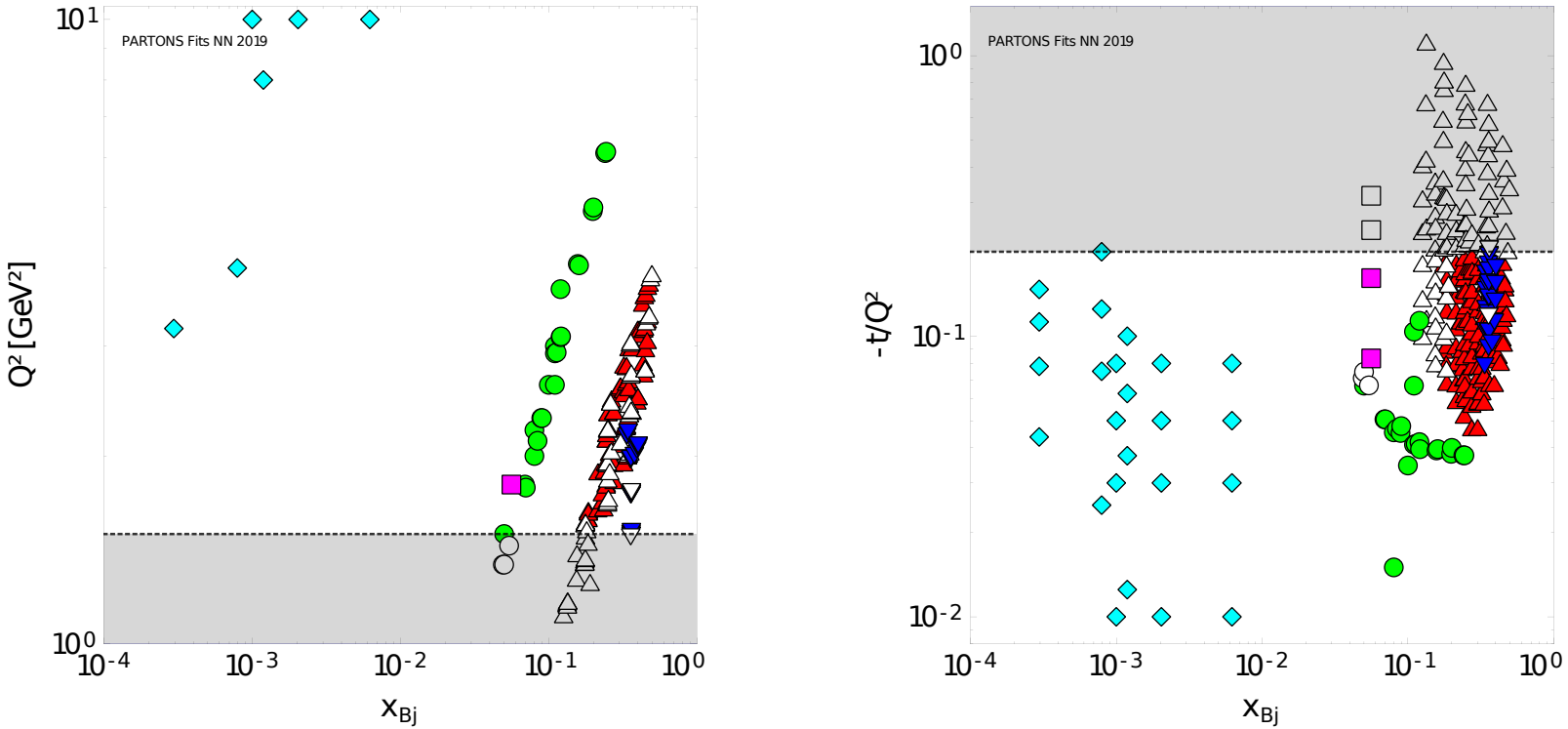

Figure: Coverage of the (x_{Bj}, Q^2) (left) and $(x_{\mathrm{Bj}}, -t/Q^2)$ (right) phase-spaces by the experimental data used in DVCS CFFs fit. The data come from the Hall A (▼, ▽), CLAS (▲, △), HERMES (●, ○), COMPASS (■, □) and HERA H1 and ZEUS (◆, ◇) experiments. The gray bands (open markers) indicate phase-space areas (experimental points) being excluded from this analysis due to the cuts.

Present experiments

- JLAB 12 GeV upgrade. Hall A and CLAS measure beam spin and target spin asymmetries with much higher luminosity, smaller x_B and higher Q^2. Hall A and CLAS measure DVCS on neutron (deuterium) necessary to make GPD flavour separation.
- COMPASS - recoil detector to ensure exclusivity - measure mixed charge-spin asymmetries with $160\,\mathrm{GeV}$ muon beam.

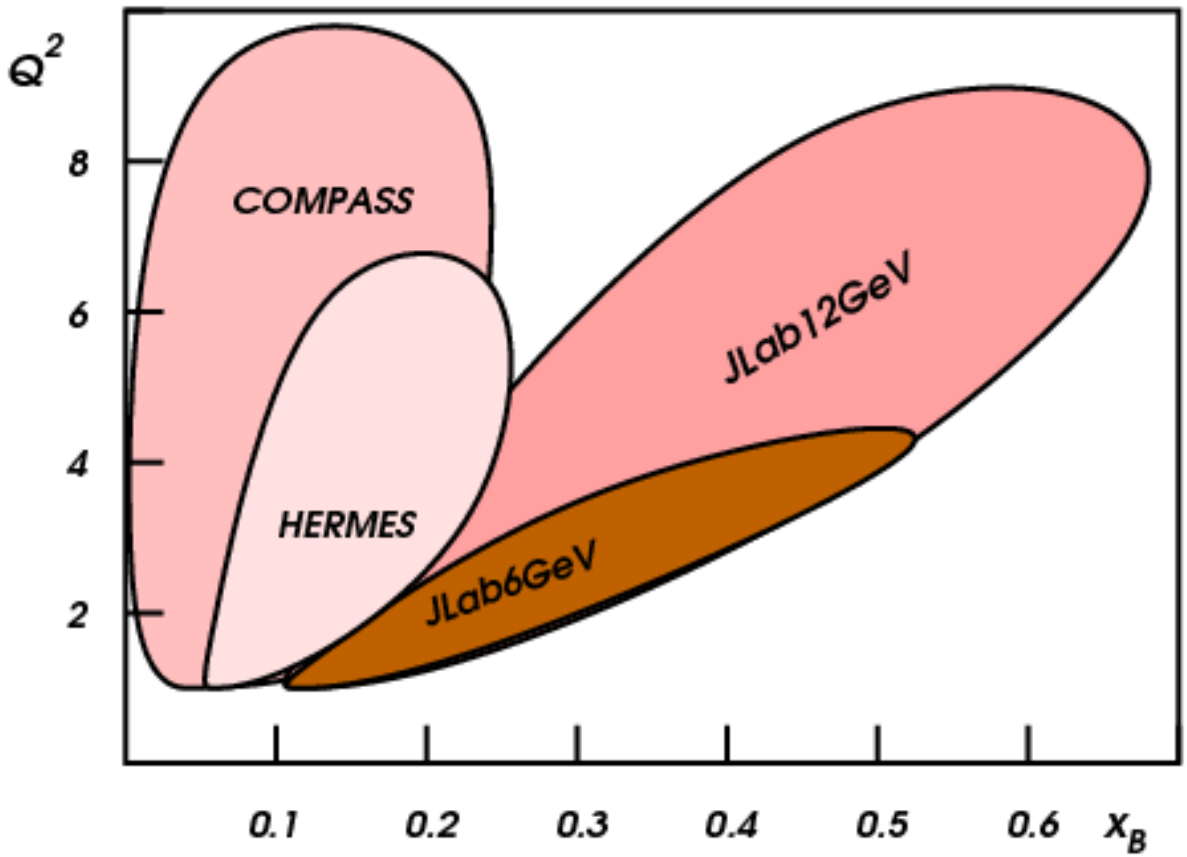

EIC - kinematic coverage for exclusive processes

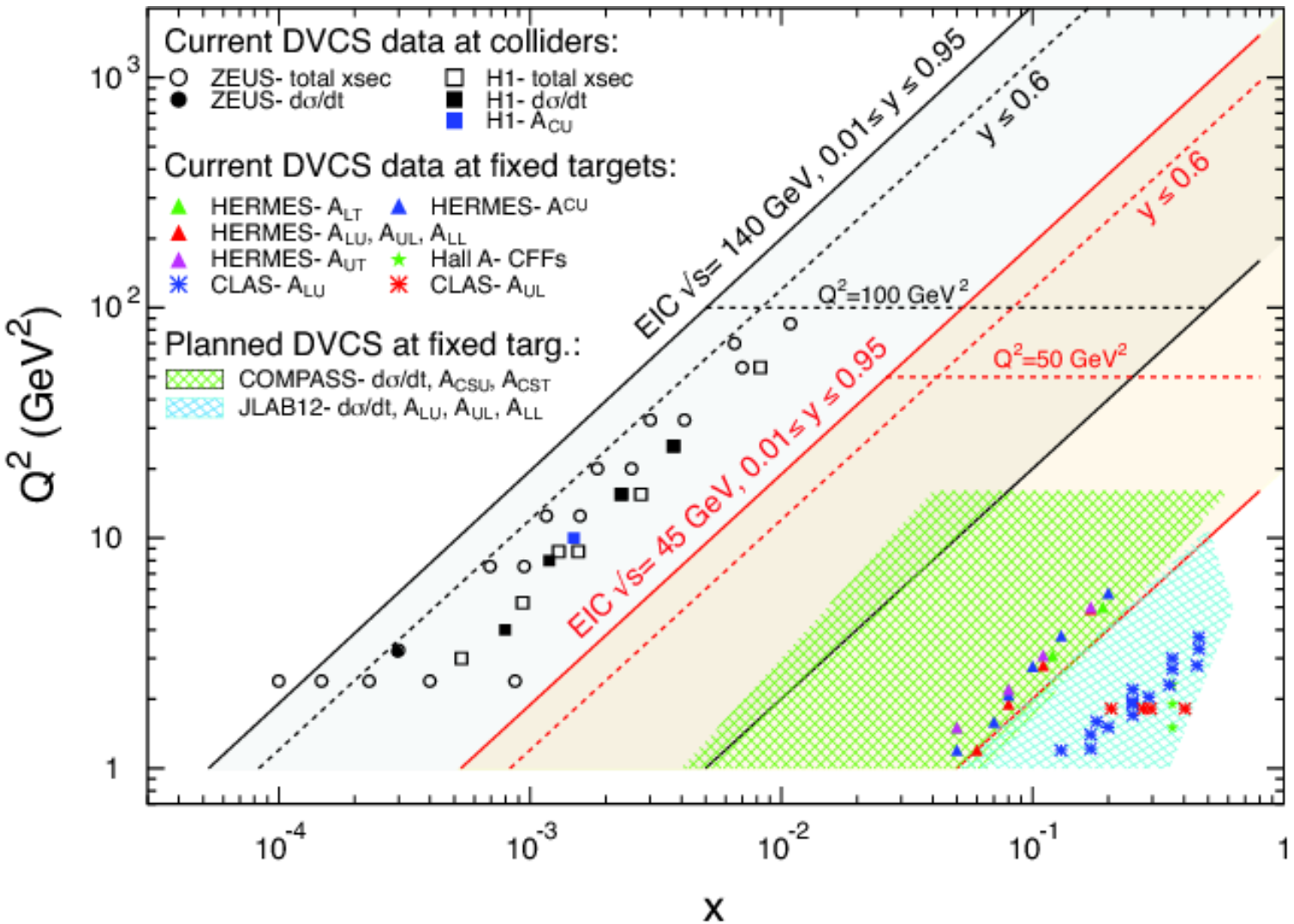

Exclusive processes and GPDs

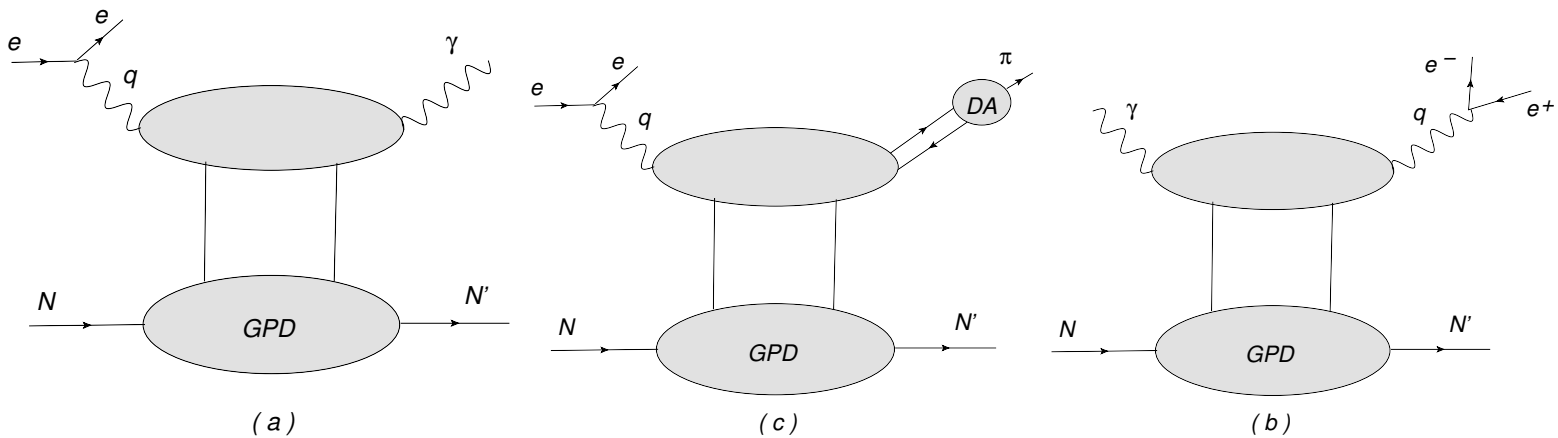

- Various exclusive processes give information about GPDs: DVCS, TCS, DDVCS, DVMP, HVMP

So, in addition to spacelike DVCS ...

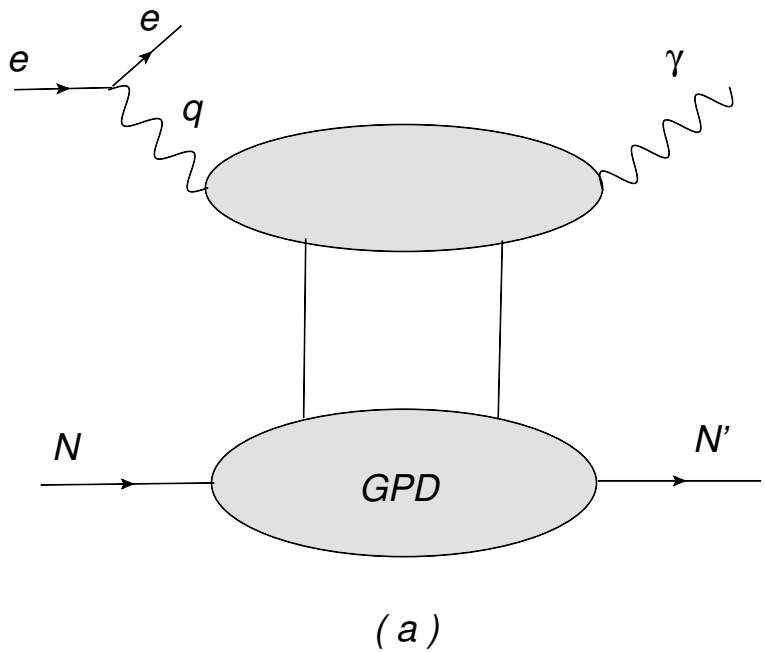

Figure: Deeply Virtual Compton Scattering (DVCS) : $lN \to l'N'\gamma$

we MUST also study timelike DVCS

Berger, Diehl, Pire, 2002

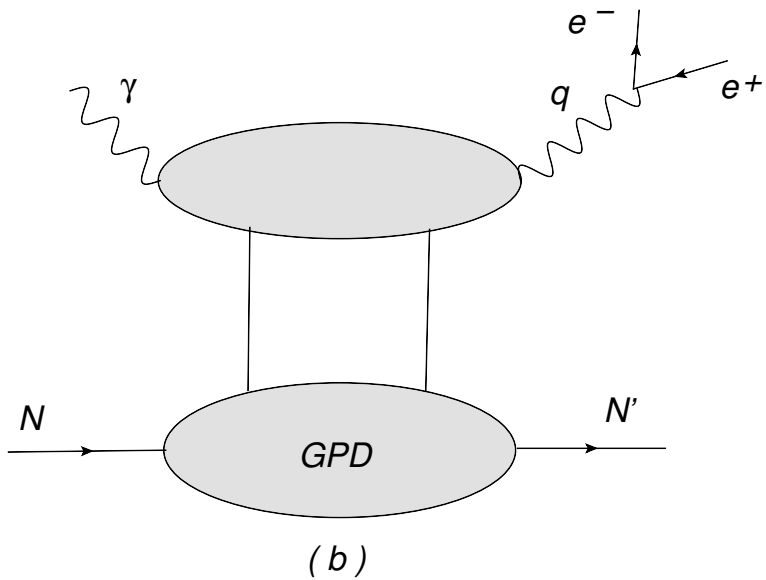

Figure: Timelike Compton Scattering (TCS): $\gamma N \to l^+ l^- N'$

Why TCS:

- same proven factorization properties as DVCS
- universality of the GPDs
- another source for GPDs (special sensitivity on real part of GPD H),
- spacelike-timelike crossing (different analytic structure - cut in Q^2)

Exciting times - DATA is coming!!!

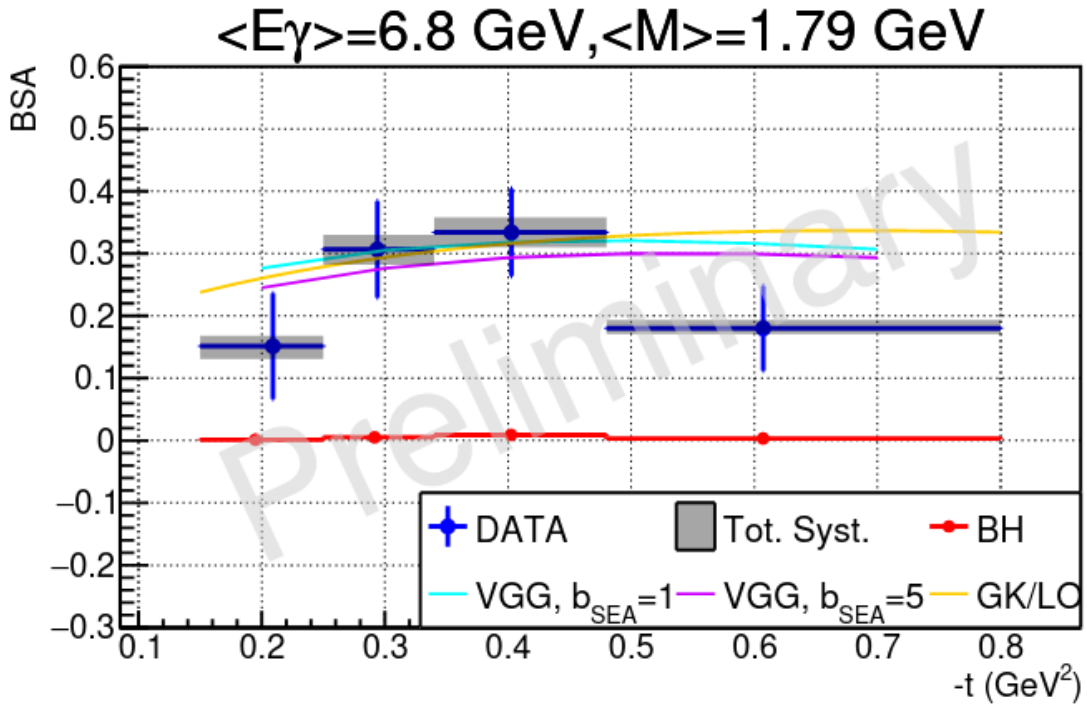

Figure 6.14: CLAS12 data points for the TCS BSA as a function of $-t$, evaluated at $\phi = 90°$, integrated over CLAS12 acceptance and over all the other variables. The vertical blue error bars are statistical uncertainties while the grey bands correspond to systematic uncertainties. Three model predictions, obtained using the VGG and GK models, are also displayed. The model predictions are calculated at the mean kinematic point given above the plot. The red points are the expected values of the BSA for BH-only events, obtained using BH-weighted simulations.

Data from CLAS12 at JLab - PhD thesis of Pierre Chatagnon (2020, Orsay)

Coefficient functions and Compton Form Factors

CFFs are the GPD dependent quantities which enter the amplitudes. They are defined through relations:

$$\mathcal{A}^{\mu\nu}(\xi,t) = -e^2 \frac{1}{(P+P')^+}\,\bar{u}(P')\left[g_T^{\mu\nu}\left(\mathcal{H}(\xi,t)\,\gamma^+ + \mathcal{E}(\xi,t)\,\frac{i\sigma^{+\rho}\Delta_\rho}{2M}\right) + i\epsilon_T^{\mu\nu}\left(\widetilde{\mathcal{H}}(\xi,t)\,\gamma^+\gamma_5 + \widetilde{\mathcal{E}}(\xi,t)\,\frac{\Delta^+\gamma_5}{2M}\right)\right] u(P)\,,$$

where:

$$\begin{aligned}
\mathcal{H}(\xi,t) &= +\int_{-1}^{1} dx \left(\sum_q T^q(x,\xi)H^q(x,\xi,t) + T^g(x,\xi)H^g(x,\xi,t)\right)\\
\widetilde{\mathcal{H}}(\xi,t) &= -\int_{-1}^{1} dx \left(\sum_q \widetilde{T}^q(x,\xi)\widetilde{H}^q(x,\xi,t) + \widetilde{T}^g(x,\xi)\widetilde{H}^g(x,\xi,t)\right).
\end{aligned}$$

Spacelike vs Timelike

D.Mueller, B.Pire, L.Szymanowski, J.Wagner, Phys.Rev.D86, 2012.

Thanks to simple spacelike-to-timelike relations, we can express the timelike CFFs by the spacelike ones in the following way:

$$
\begin{aligned}
{}^{T}\mathcal{H} &\overset{\text{LO}}{=} {}^{S}\mathcal{H}^{*}\,, \\
{}^{T}\widetilde{\mathcal{H}} &\overset{\text{LO}}{=} -{}^{S}\widetilde{\mathcal{H}}^{*}\,, \\
{}^{T}\mathcal{H} &\overset{\text{NLO}}{=} {}^{S}\mathcal{H}^{*} - i\pi\,\mathcal{Q}^{2}\frac{\partial}{\partial\mathcal{Q}^{2}}{}^{S}\mathcal{H}^{*}\,, \\
{}^{T}\widetilde{\mathcal{H}} &\overset{\text{NLO}}{=} -{}^{S}\widetilde{\mathcal{H}}^{*} + i\pi\,\mathcal{Q}^{2}\frac{\partial}{\partial\mathcal{Q}^{2}}{}^{S}\widetilde{\mathcal{H}}^{*}\,.
\end{aligned}
$$

The corresponding relations exist for (anti-)symmetric CFFs $\mathcal{E}$ ($\widetilde{\mathcal{E}}$).

DVCS CFFs from Artificial Neural Network fit

H. Moutarde, P. Sznajder, J. Wagner, Eur.Phys.J. C79 (2019)

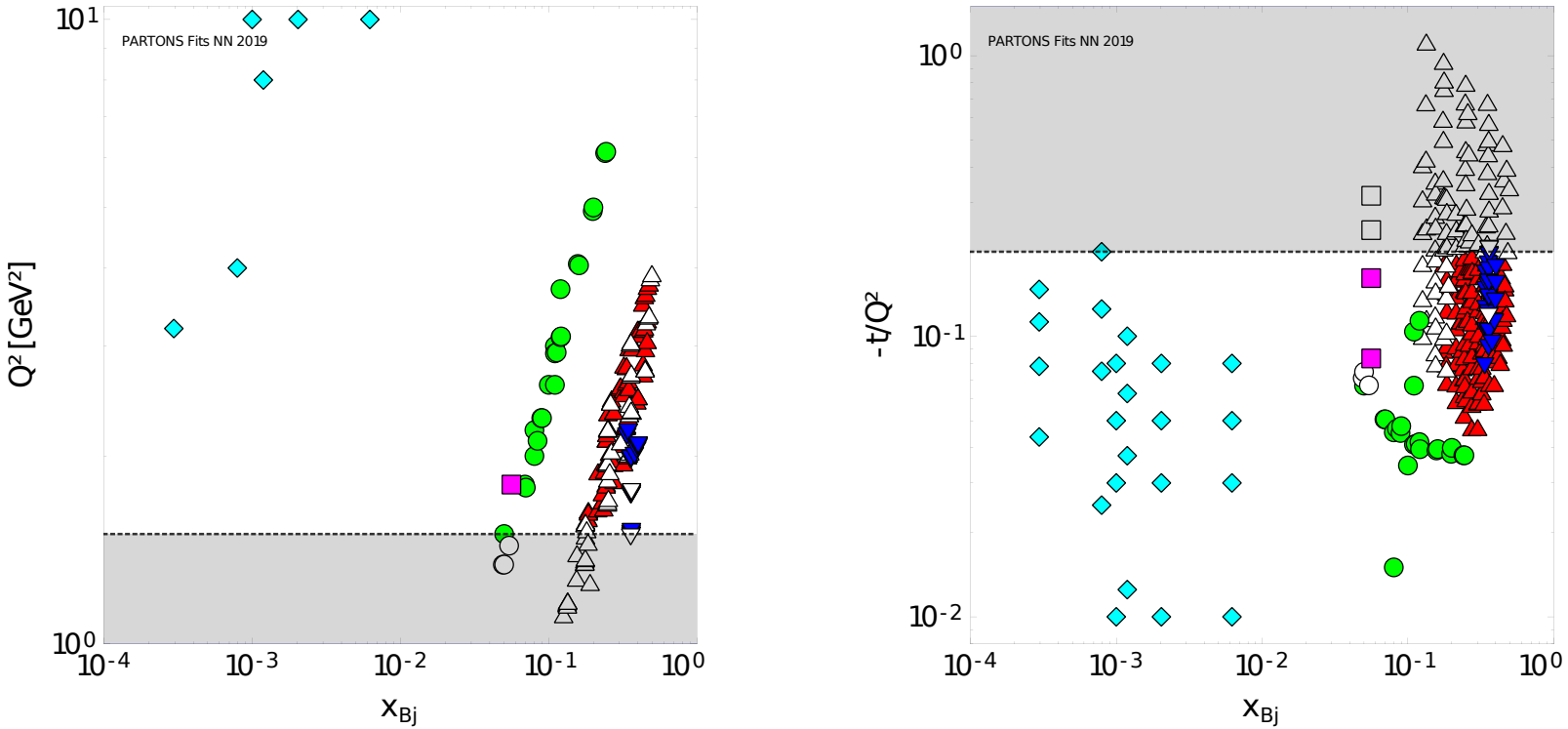

Figure: Coverage of the (x_{Bj}, Q^2) (left) and $(x_{\mathrm{Bj}}, -t/Q^2)$ (right) phase-spaces by the experimental data used in DVCS CFFs fit. The data come from the Hall A (▼, ▽), CLAS (▲, △), HERMES (●, ○), COMPASS (■, □) and HERA H1 and ZEUS (◆, ◇) experiments. The gray bands (open markers) indicate phase-space areas (experimental points) being excluded from this analysis due to the cuts.

DVCS vs TCS CFFs

O. Grocholski, H. Moutarde, B. Pire, P. Sznajder, J. Wagner, Eur.Phys.J. C80 (2020)

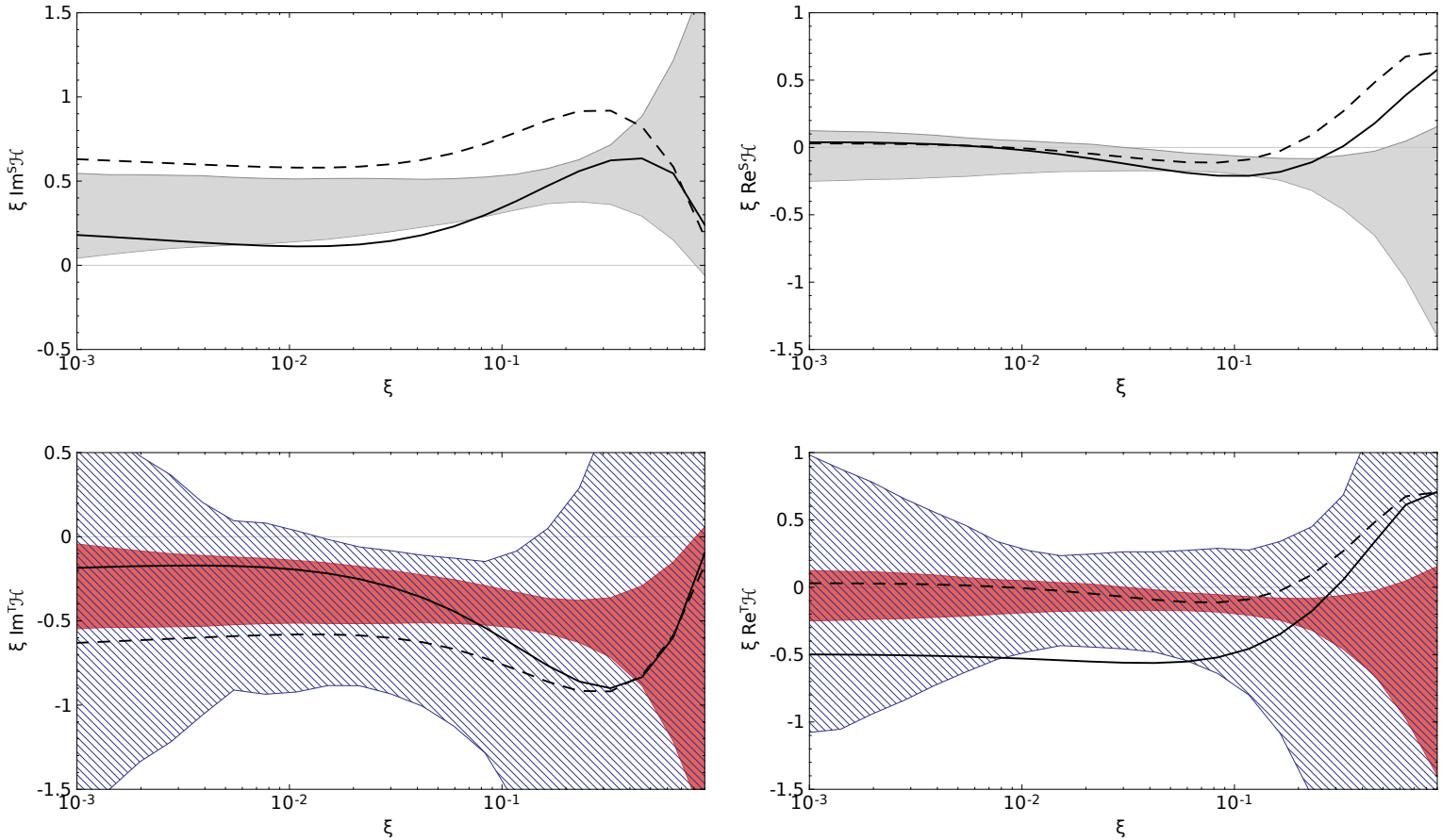

Figure: Imaginary (left) and real (right) part of DVCS (up) and TCS (down) CFF for $Q^2 = 2$ GeV^2 and $t = -0.3$ GeV^2 as a function of ξ. The shaded red (dashed blue) bands correspond to the data-driven predictions coming from the ANN global fit of DVCS data and they are evaluated using LO (NLO) spacelike-to-timelike relations. The dashed (solid) lines correspond to the GK GPD model evaluated with LO (NLO) coefficient functions.

TCS and Bethe-Heitler contribution to exclusive lepton pair photoproduction.

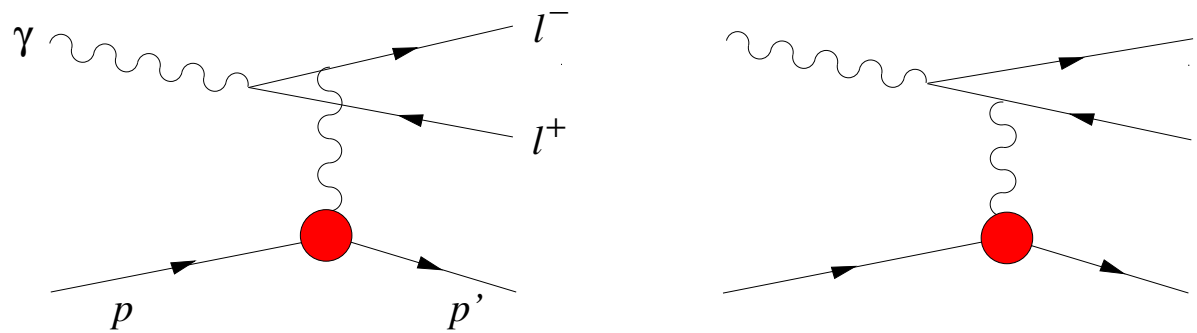

Figure: The Feynman diagrams for the Bethe-Heitler amplitude.

The cross-section for photoproduction of a lepton pair:

$$\frac{d\sigma}{dQ'^2\ dt\ d\phi\ d\cos\theta} = \frac{d\left(\sigma_{\rm BH} + \sigma_{\rm TCS} + \sigma_{\rm INT}\right)}{dQ'^2\ dt\ d\phi\ d\cos\theta}$$

Berger, Diehl, Pire, 2002

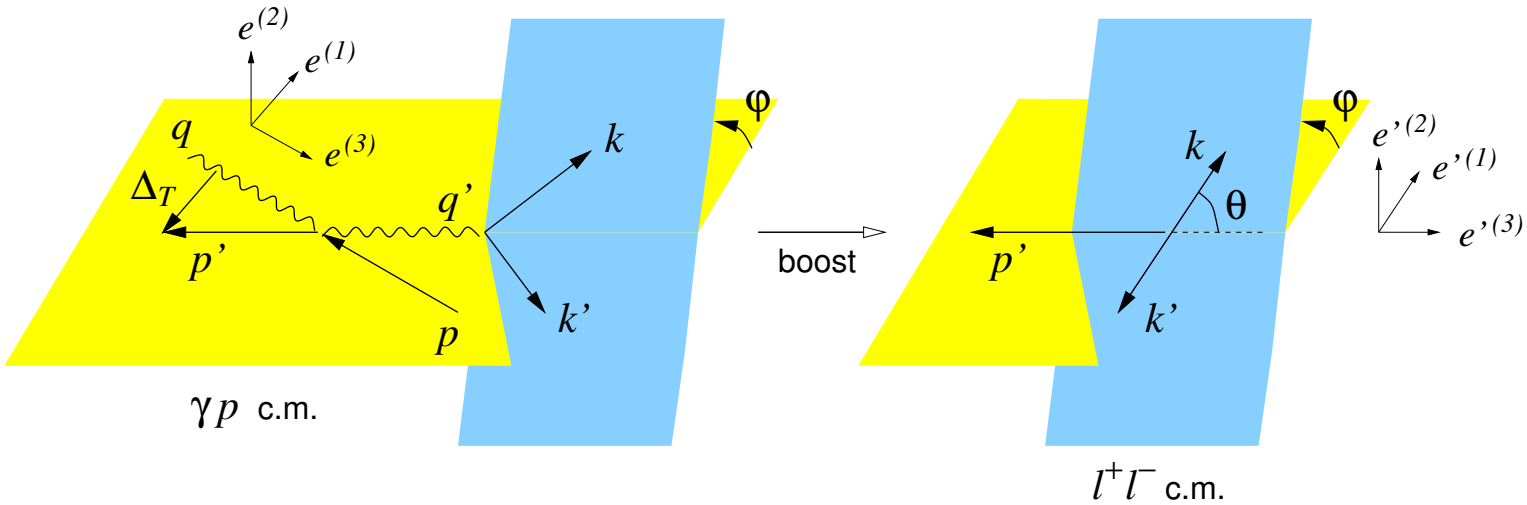

Figure: Kinematical variables and coordinate axes in the γp and $\ell^+\ell^-$ c.m. frames.

$$\frac{d\sigma}{dQ'^2\ dt\ d\phi\ d\cos\theta}$$

- Important to measure ϕ !
- BH dominates at θ close to 0 and π !

Interference

- B-H dominant for not very high energies (JLAB), at higher energies the TCS/BH ratio is bigger due to growth of the gluon and sea densities.

Pire, Szymanowski, JW PRD 83

Moutarde, Pire, Sabatié, Szymanowski, JW PRD 87

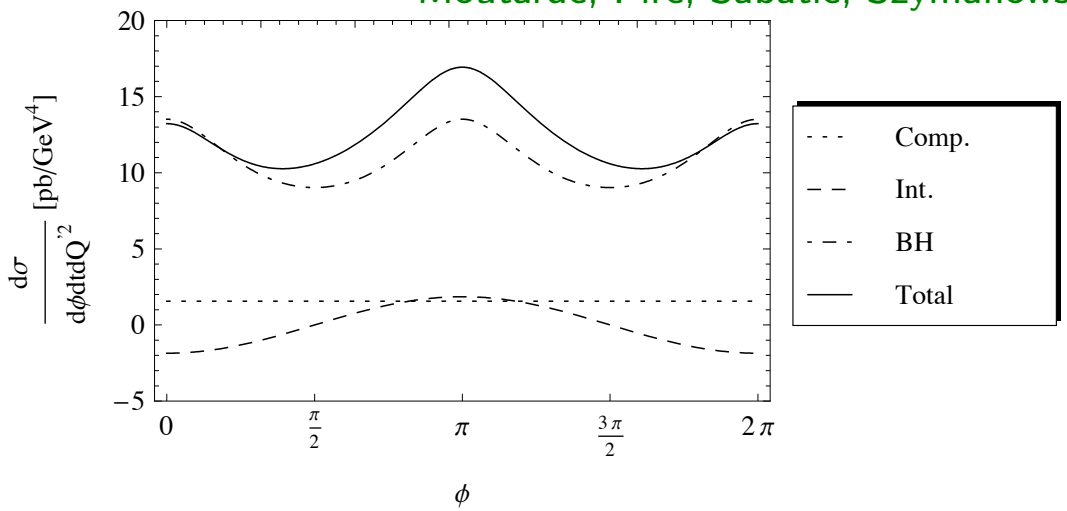

Figure: The differential cross section for $t = -0.2$ GeV^2 , $Q'^2 = 5$ GeV^2 , and integrated over $\theta \in (\pi/4, 3\pi/4)$ as a function of ϕ, for $s = 10^3$ GeV^2.

- The interference part of the cross-section for $\gamma p \to \ell^+\ell^- p$ with unpolarized protons and photons is given by:

$$\frac{d\sigma_{INT}}{dQ'^2\, dt\, d\cos\theta\, d\varphi} \sim \cos\varphi \cdot \ \mathrm{Re}\,\mathcal{H}(\xi, t) \leftarrow \text{Sensitivity to the D-term!}$$

Charge asymmetry selects interference - in DVCS one needs positron beam, here this is given by the angular dependence!

Interference

R ratio:

$$R = \frac{2\int_0^{2\pi} \cos\phi \; d\phi \int_{\pi/4}^{3\pi/4} d\theta \frac{dS}{dQ'^2 dt d\phi d\theta}}{\int_0^{2\pi} d\phi \int_{\pi/4}^{3\pi/4} d\theta \frac{dS}{dQ'^2 dt d\phi d\theta}} ,$$

where S is the weighted cross section :

$$\frac{dS}{dQ'^2 dt d\phi d\theta} = \frac{L(\theta,\phi)}{L_0(\theta)} \frac{d\sigma}{dQ'^2 dt d\phi d\theta} ,$$

Asymmetry (Chatagnon & Vanderhaeghen):

$$A_{FB}(\theta,\phi) = \frac{d\sigma(\theta,\phi) - d\sigma(180^\circ - \theta, 180^\circ + \phi)}{d\sigma(\theta,\phi) + d\sigma(180^\circ - \theta, 180^\circ + \phi)}$$

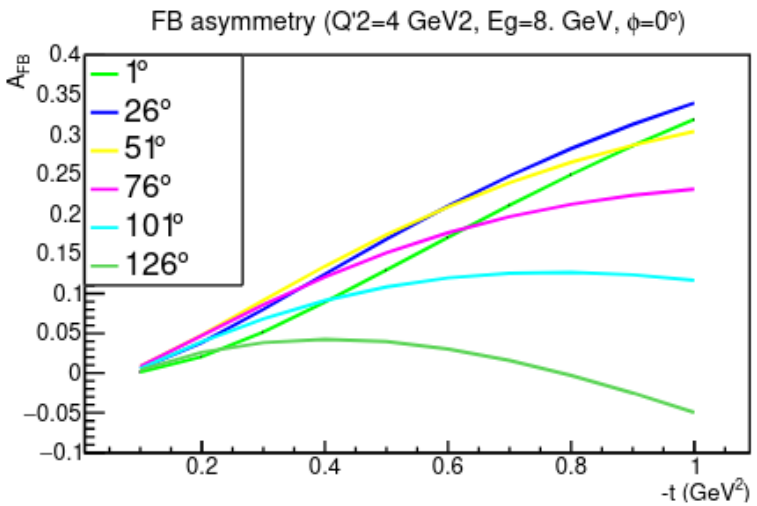

(a)

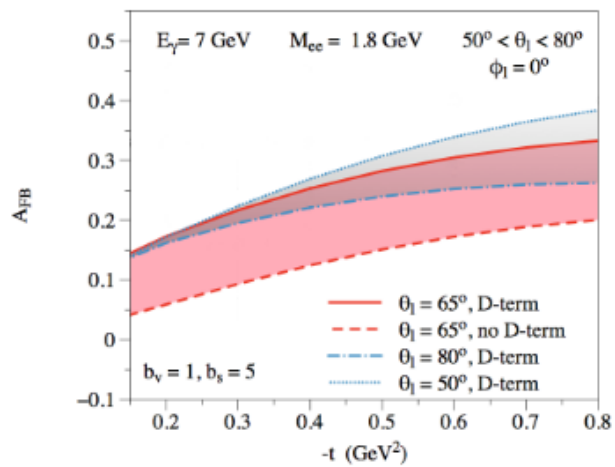

(b)

Unpolarized cross section

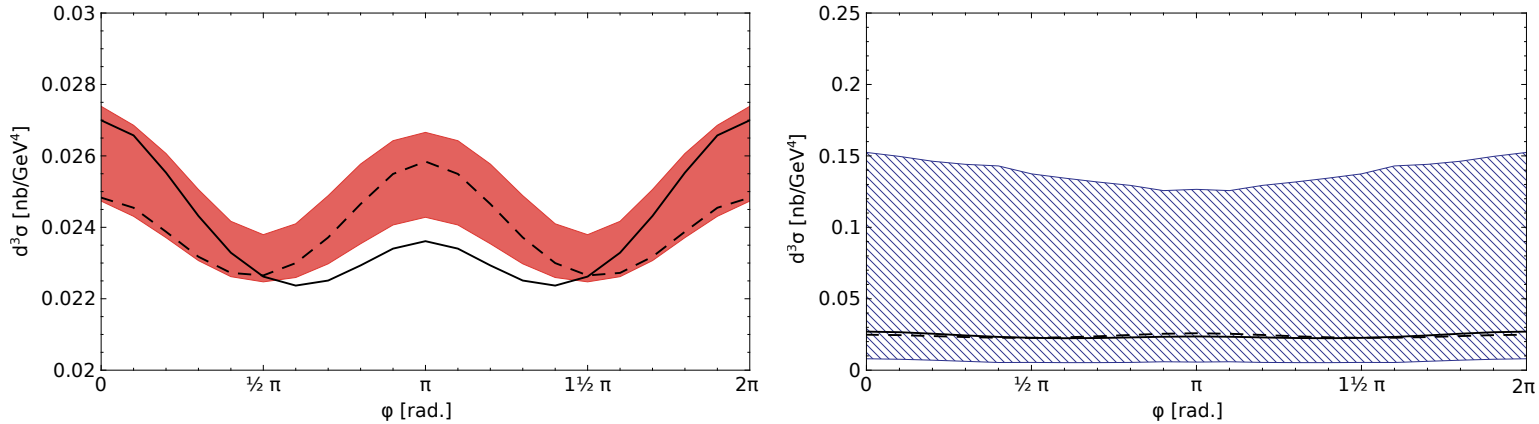

Figure: Differential TCS cross section integrated over $\theta \in (\pi/4, 3\pi/4)$ for $Q'^2 = 4$ GeV^2, $t = -0.1$ GeV^2 and the photon beam energy $E_\gamma = 10$ GeV as a function of the angle ϕ. In the left (right) panel the data-driven predictions evaluated using LO (NLO) spacelike-to-timelike relations are shown. The dashed (solid) lines correspond to the GK GPD model evaluated with LO (NLO) TCS coefficient functions (the curves are the same in both panels). Note the different scales for the upper and lower panels.

R ratio

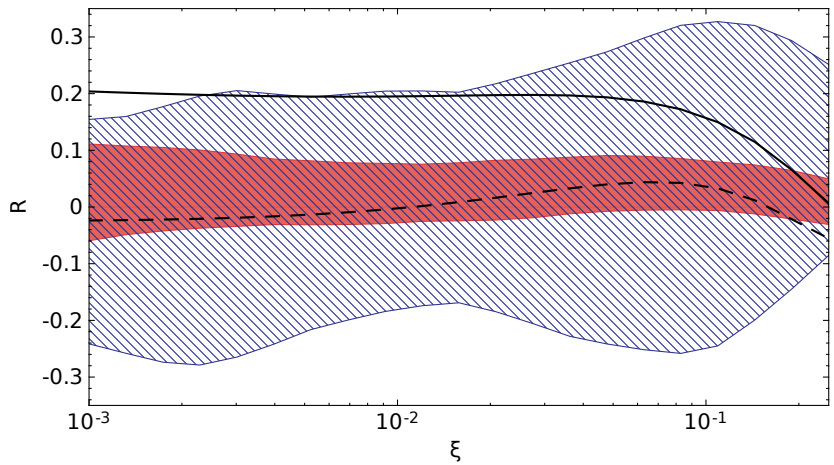

Figure: Ratio R evaluated with LO and NLO spacelike-to-timelike relations for $Q'^2 = 4$ GeV^2, $t = -0.35$ GeV^2 as a function of ξ.

Circular asymmetry

The photon beam circular polarization asymmetry:

$$A_{CU} = \frac{\sigma^+ - \sigma^-}{\sigma^+ + \sigma^-} \sim Im(H)$$

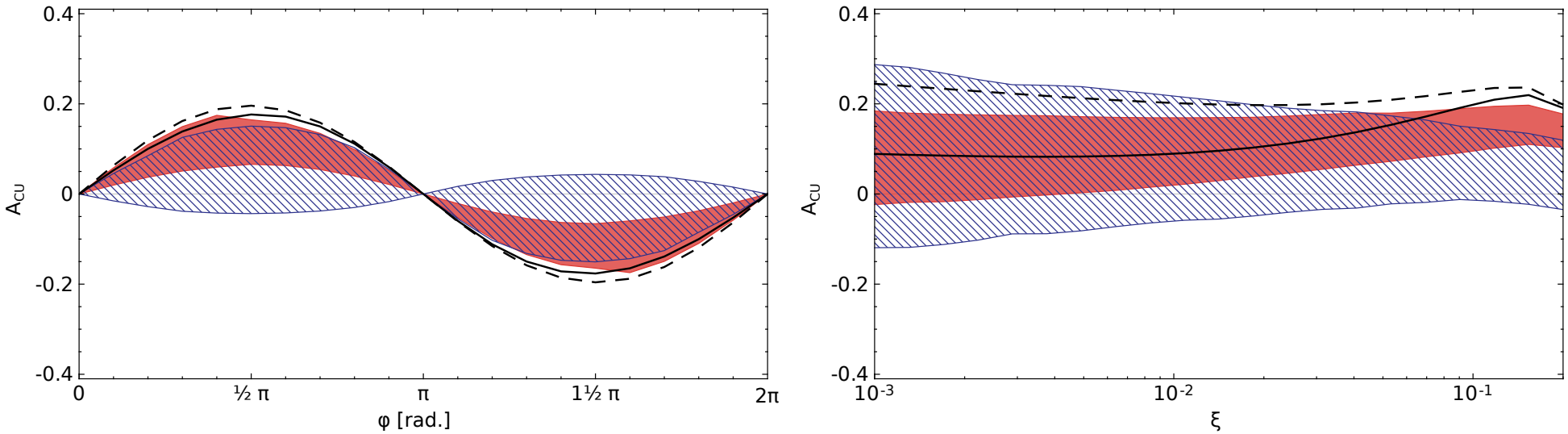

Figure: Circular asymmetry A_{CU} evaluated with LO and NLO spacelike-to-timelike relations for $Q'^2 = 4$ GeV^2, $t = -0.1$ GeV^2 and (left) $E_\gamma = 10$ GeV as a function of ϕ (right) and $\phi = \pi/2$ as a function of ξ. The cross sections used to evaluate the asymmetry are integrated over $\theta \in (\pi/4, 3\pi/4)$.

Transverse target asymmetry

$$\frac{d\sigma_{\mathrm{INT}}^{\mathrm{tpol}}}{dQ'^2 d(\cos\theta) d\phi dt d\varphi_S} \sim \sin\varphi_S \Im\Big[\mathcal{H} - \frac{\xi^2}{1-\xi^2}\mathcal{E} + \widetilde{\mathcal{H}} + \frac{t}{4M^2}\widetilde{\mathcal{E}}\Big]. \qquad (1)$$

The transverse spin asymmetry:

$$A_{UT}(\varphi_S) = \frac{\sigma(\varphi_S) - \sigma(\varphi_S - \pi)}{\sigma(\varphi_S) + \sigma(\varphi_S - \pi)}, \qquad (2)$$

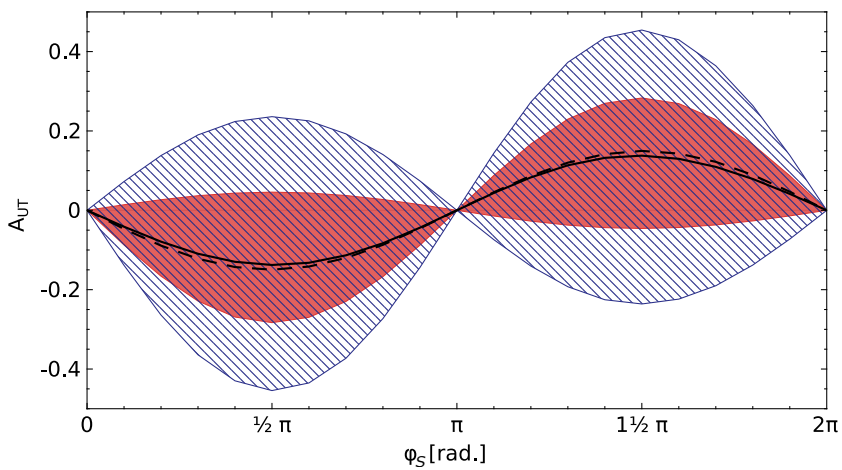

Figure: Transverse target spin asymmetry A_{UT} evaluated with LO and NLO spacelike-to-timelike relations for $Q'^2 = 4$ GeV^2, $t = t_0$ and $E_\gamma = 10$ GeV as a function of φ_S. The cross sections used to evaluate the asymmetry are integrated over $\theta \in (\pi/4, 3\pi/4)$.

Experimental status

Rafayel Paremuzyan PhD thesis

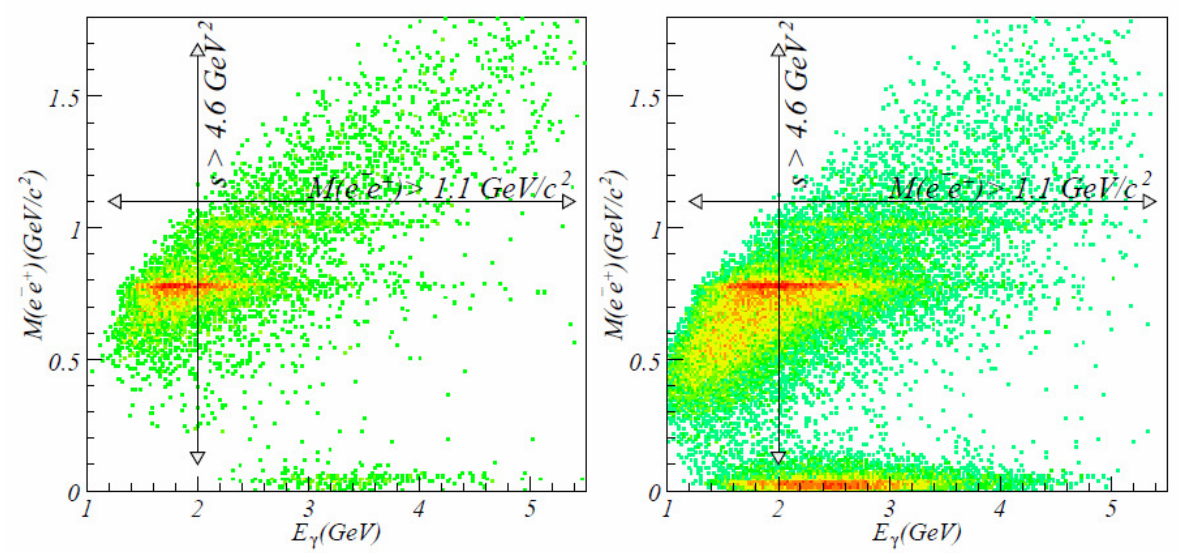

Figure: e^+e^- invariant mass distribution vs quasi-real photon energy. For TCS analysis $M(e^+e^-) > 1.1\,\mathrm{GeV}$ and $s_{\gamma p} > 4.6\,\mathrm{GeV}^2$ regions are chosen. Left graph represents e1-6 data set, right one is from e1f data set.

Experimental status

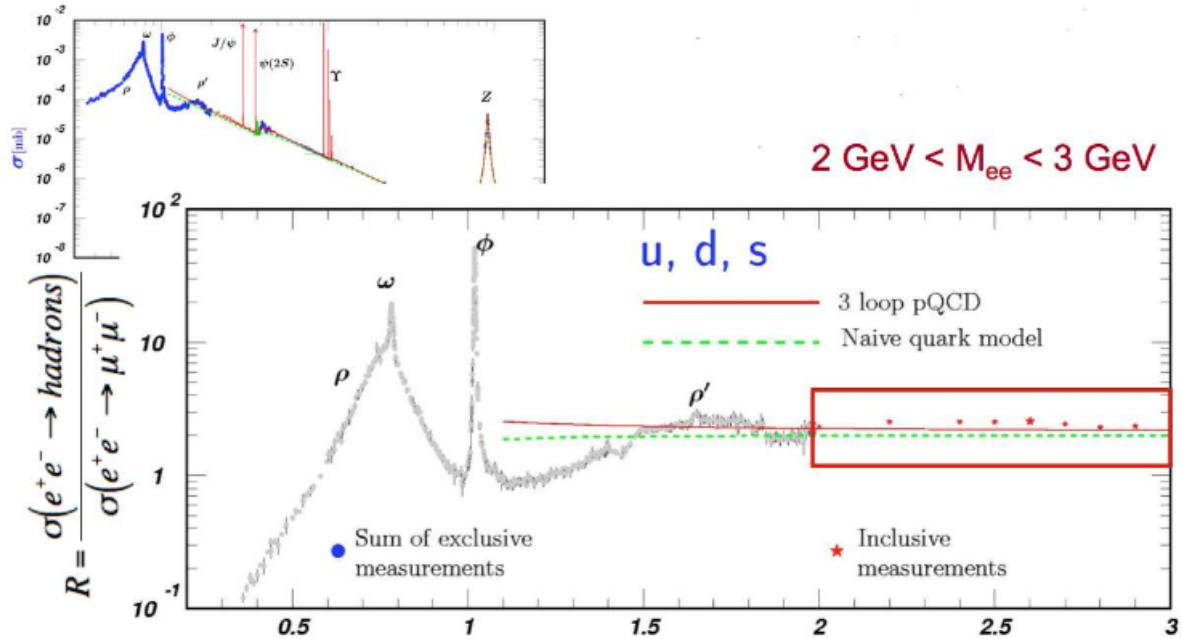

FIG. 4: Measurements of e^+e^- annihilation into hadrons show a resonance-free window between the ρ' and the J/ψ, which is ideal for TCS studies at 12 GeV.

- CLAS - E12-12-001 : Preliminary results in the Pierre Chatagnon PhD thesis !

Experimental prospects - Ultraperipheral collisions

B.Pire, L.Szymanowski, J.Wagner, PRD86

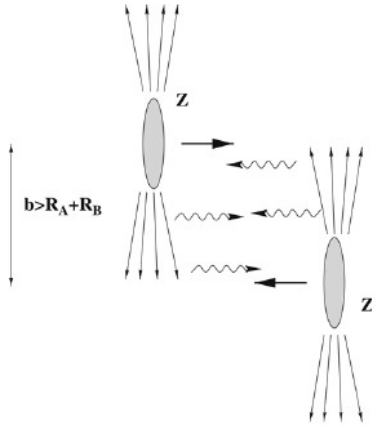

$$\sigma^{AB} = \int dk_A \frac{dn^A}{dk_A} \sigma^{\gamma B}(W_A(k_A)) + \int dk_B \frac{dn^B}{dk_B} \sigma^{\gamma A}(W_B(k_B))$$

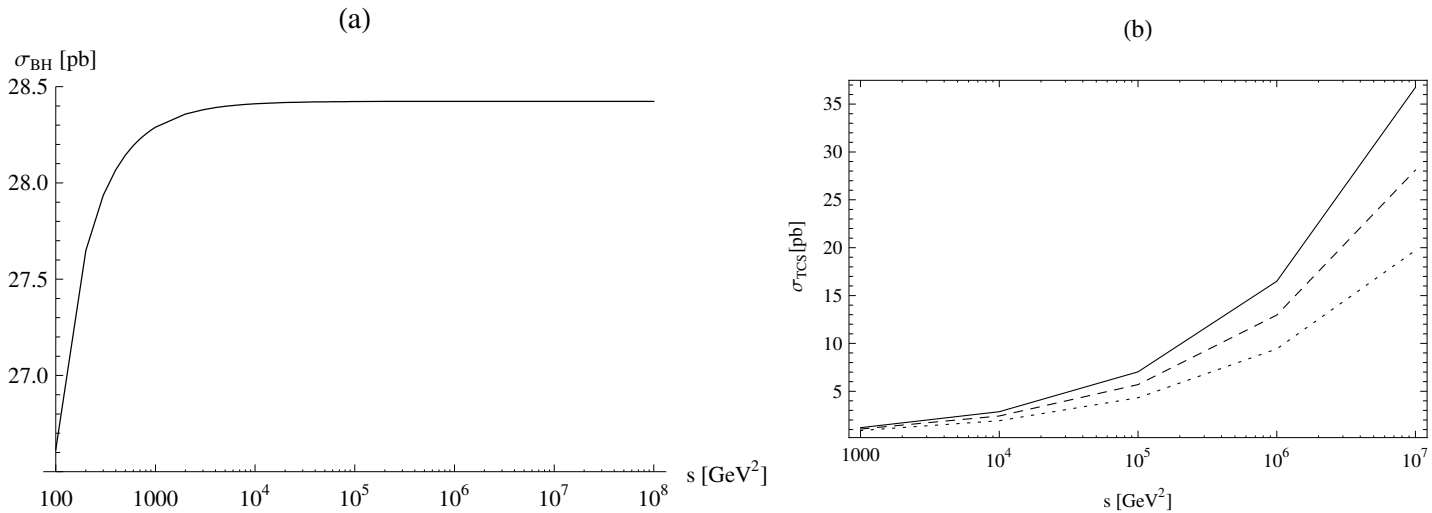

Figure: (a) The BH cross section (b) σ_{TCS} as a function of γp c.m. energy squared s

Yellow Report:

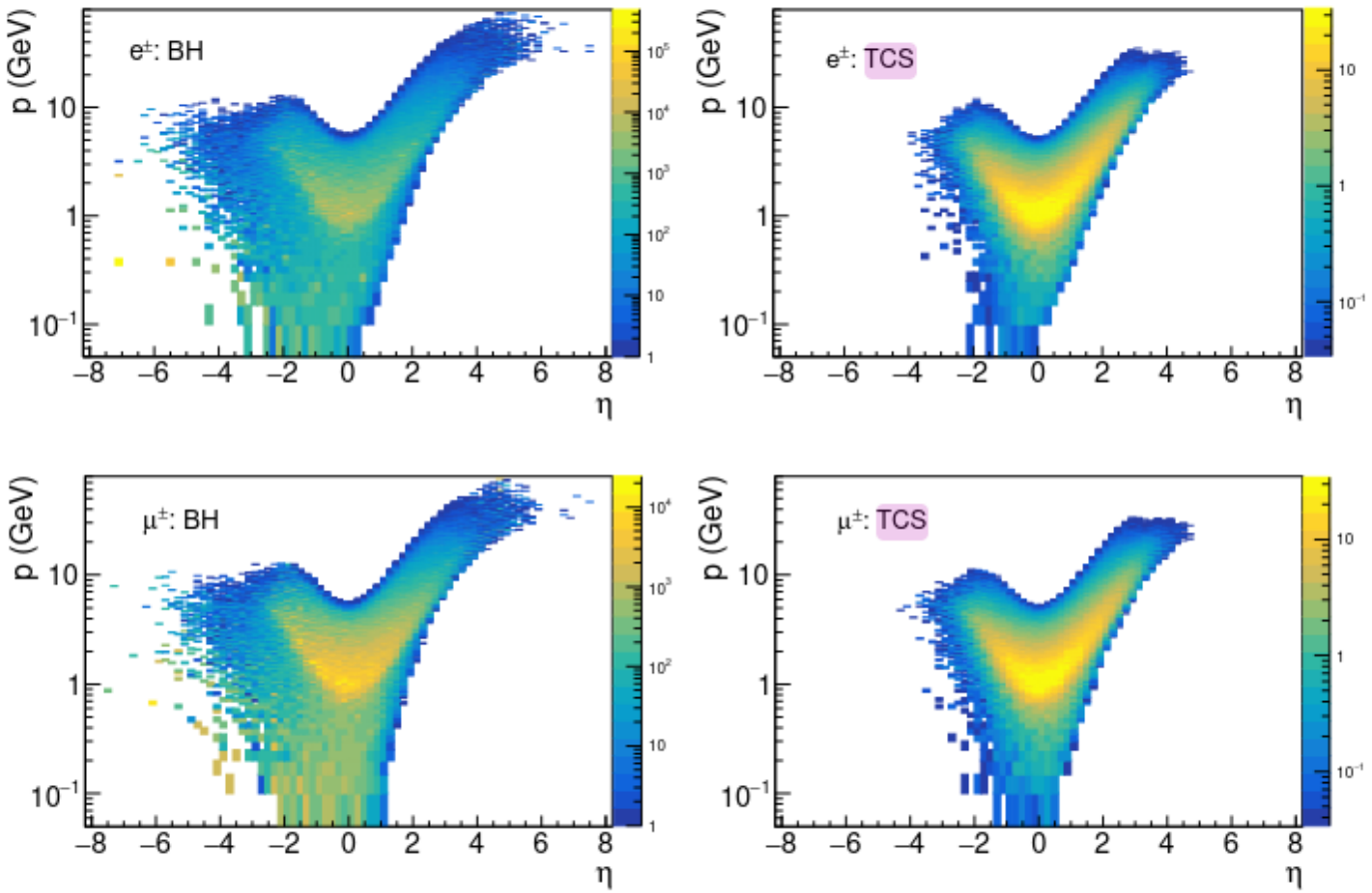

Figure 8.69: Momentum vs pseudorapidity for e^+e^- (top) and $\mu^+\mu^-$ (bottom) at the 5×41 GeV collision energy, for an integrated luminosity of 10 fb^{-1}. Left: BH, right: TCS.

More detailed analysis under way: Kayleigh Gates, Daria Sokhan.

General Compton Scattering:

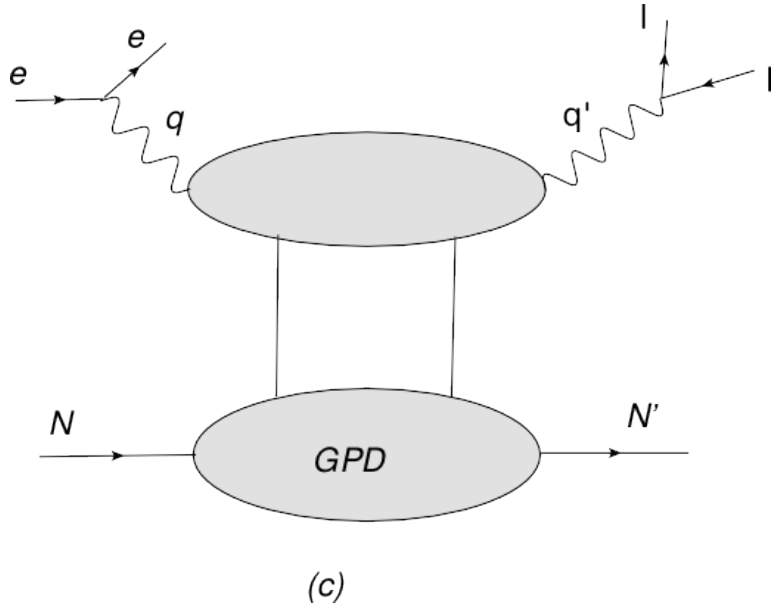

Figure: Double Deeply Virtual Compton Scattering (DDVCS): $\gamma N \to l^+ l^- N'$

$$\gamma^*(q_{in})N(p) \to \gamma^*(q_{out})N'(p')$$

variables, describing the processes of interest in this generalized Bjorken limit, are the scaling variable ξ and skewness $\eta > 0$:

$$\xi = -\frac{q_{out}^2 + q_{in}^2}{q_{out}^2 - q_{in}^2}\eta\,, \quad \eta = \frac{q_{out}^2 - q_{in}^2}{(p+p')\cdot(q_{in}+q_{out})}\,.$$

- DDVCS: $q_{in}^2 < 0\,, \quad q_{out}^2 > 0\,, \quad \eta \neq \xi$
- DVCS: $q_{in}^2 < 0\,, \quad q_{out}^2 = 0\,, \quad \eta = \xi > 0$
- TCS: $q_{in}^2 = 0\,, \quad q_{out}^2 > 0\,, \quad \eta = -\xi > 0$

Coefficient functions and Compton Form Factors

CFFs are the GPD dependent quantities which enter the amplitudes. They are defined through relations:

$$\mathcal{A}^{\mu\nu}(\xi,\eta,t) = -e^2 \frac{1}{(P+P')^+}\,\bar{u}(P')\Bigg[g_T^{\mu\nu}\left(\mathcal{H}(\xi,\eta,t)\,\gamma^+ + \mathcal{E}(\xi,\eta,t)\,\frac{i\sigma^{+\rho}\Delta_\rho}{2M}\right) + i\epsilon_T^{\mu\nu}\left(\widetilde{\mathcal{H}}(\xi,\eta,t)\,\gamma^+\gamma_5 + \widetilde{\mathcal{E}}(\xi,\eta,t)\,\frac{\Delta^+\gamma_5}{2M}\right)\Bigg] u(P)\,,$$

,where:

$$\begin{aligned}
\mathcal{H}(\xi,\eta,t) &= +\int_{-1}^{1} dx \left(\sum_q T^q(x,\xi,\eta)H^q(x,\eta,t) + T^g(x,\xi,\eta)H^g(x,\eta,t)\right)\\
\widetilde{\mathcal{H}}(\xi,\eta,t) &= -\int_{-1}^{1} dx \left(\sum_q \widetilde{T}^q(x,\xi,\eta)\widetilde{H}^q(x,\eta,t) + \widetilde{T}^g(x,\xi,\eta)\widetilde{H}^g(x,\eta,t)\right).
\end{aligned}$$

LO

- DVCS vs TCS

$$
\begin{aligned}
{}^{DVCS}T^q &= -e_q^2 \tfrac{1}{x+\eta-i\varepsilon} - (x \to -x) = \quad ({}^{TCS}T^q)^* \\
{}^{DVCS}\tilde{T}^q &= -e_q^2 \tfrac{1}{x+\eta-i\varepsilon} + (x \to -x) = \quad -({}^{TCS}\tilde{T}^q)^*
\end{aligned}
$$

$$
{}^{DVCS}Re(\mathcal{H}) \sim P \int \frac{1}{x \pm \eta} H^q(x,\eta,t)\,, \qquad {}^{DVCS}Im(\mathcal{H}) \sim i\pi H^q(\pm\eta,\eta,t)
$$

- DDVCS

$$
{}^{DDVCS}T^q = -e_q^2 \frac{1}{x+\xi-i\varepsilon} - (x \to -x)
$$

$$
{}^{DDVCS}Re(\mathcal{H}) \sim P \int \frac{1}{x \pm \xi} H^q(x,\eta,t)\,, \qquad {}^{DVCS}Im(\mathcal{H}) \sim i\pi H^q(\pm\xi,\eta,t)
$$

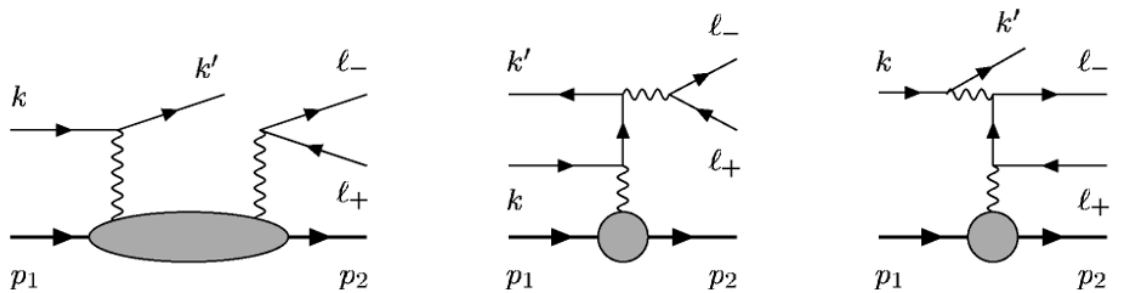

NLO analysis and pheno in progress with K. Deja, V. Martinez-Fernandez, PSz, LSz, BP

Gluon GPDs in the UPC production of heavy mesons

D. Yu. Ivanov , A. Schafer , L. Szymanowski and G. Krasnikov - **Eur.Phys.J. C34**

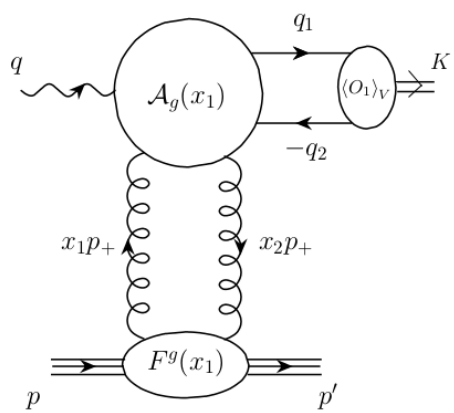

Figure 1: Kinematics of heavy vector meson photoproduction.

The amplitude $\mathcal{M}$ is given by factorization formula:

$$\mathcal{M} \sim \left(\frac{\langle O_1 \rangle_V}{m^3}\right)^{1/2} \int_{-1}^{1} dx \left[T_g(x,\xi)\, F^g(x,\xi,t) + T_q(x,\xi) F^{q,S}(x,\xi,t) \right] ,$$

$$F^{q,S}(x,\xi,t) = \sum_{q=u,d,s} F^q(x,\xi,t)\,.$$

where m is a pole mass of heavy quark, $\langle O_1 \rangle_V$ is given by NRQCD through leptonic meson decay rate.

Heavy Vector Mesons Photoproduction

Alice, The EPJC 79, 402 (2019)

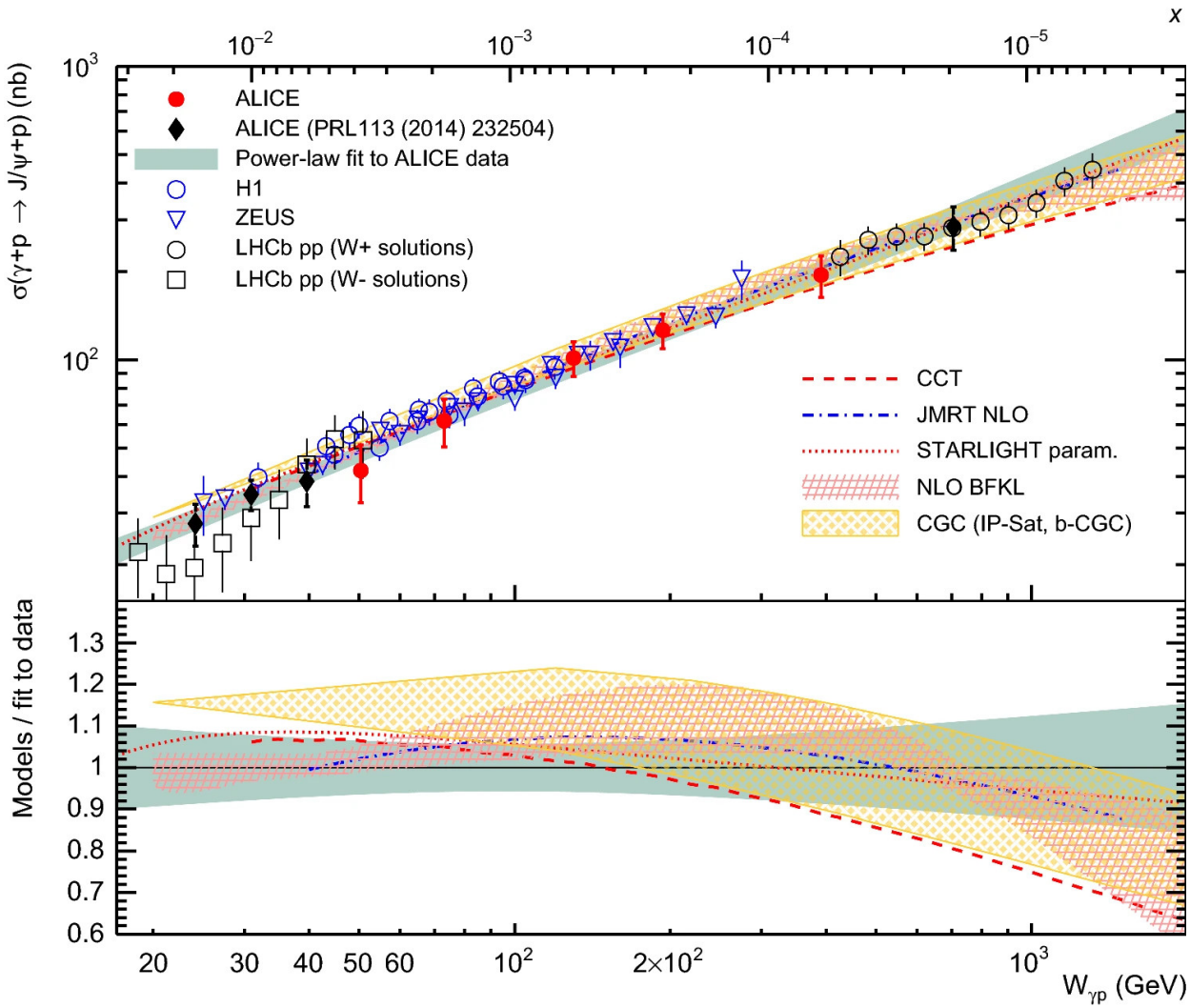

Other processes

- Light meson electroproduction:
  - sensitivity to different combinations of GPDs
  - flavor separation
- Charged current exclusive processes:
  - different combinations of GPDs due to the charged current coupling structure.
  - Much smaller cross sections, but in the reach of EIC.
- Production of two particles:
  - 2 photons
  - photon + meson
  - 2 mesons

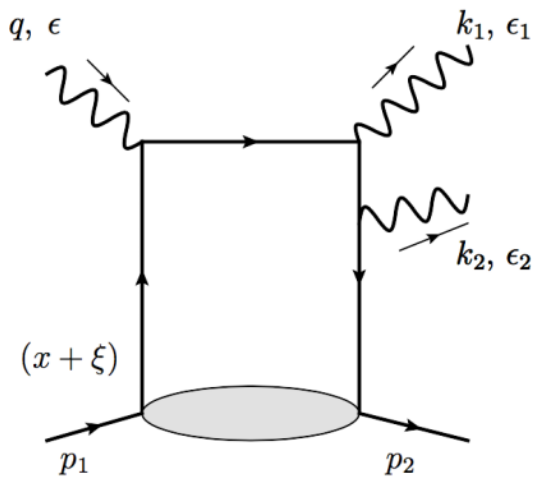

Check recent Oskar Grocholski talk at DIS2021, about factorization studies at NLO.

PARTONS

Motivation

- New precise experiments
- Various models, schemes, processes, observables
- Extraction of GPDs is complicated - various channels needed
- Various approaches: local and global CFF fitting, GPDs fitting...,
- Extrapolation for tomography (uncerteinties propagation),
- Various groups doing usually one chain

PARTONS

Structure

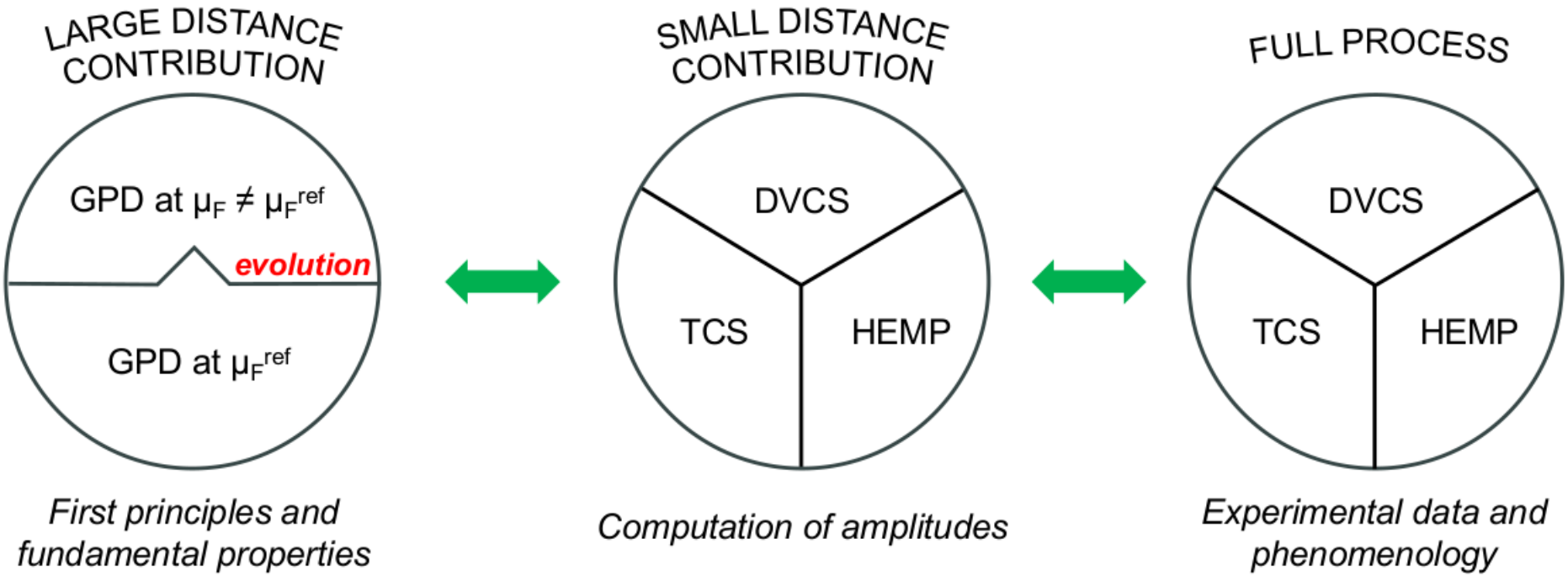

First principles and fundamental properties

Computation of amplitudes

Experimental data and phenomenology

Tasks and challenges:

- Physical models
- Perturbative approximations
- Many observables
- Numerical methods
- Accuracy and speed
- Fits

PARTONS

Existing modules

- GPD models: Goloskokov-Kroll, VGG, Vinnikov, MPSSW13, MMS13,
- Evolution: Vinnikov,
- Compton Form Factors (generally: convolution of GPDs or DA with coefficient functions): LO, NLO, NLO + heavy quarks (Noritsch)
- Cross section (DVCS + BH, TCS, π^0 meson production)
- Observables: A_{LU}, A_{UL}, A_{LL}, A_C, fourier moments, ...
- Running coupling: 4-loop PDG expression, constant value

PARTONS

- Open source
- Virtual Machine with out-of-the-box running PARTONS (also possible to install on your own Linux or Mac)
- Examples: xml, c++ codes
- Description in Eur.Phys.J. C78 (2018) no.6, 478
- Website with detailed manual: http://partons.cea.fr/

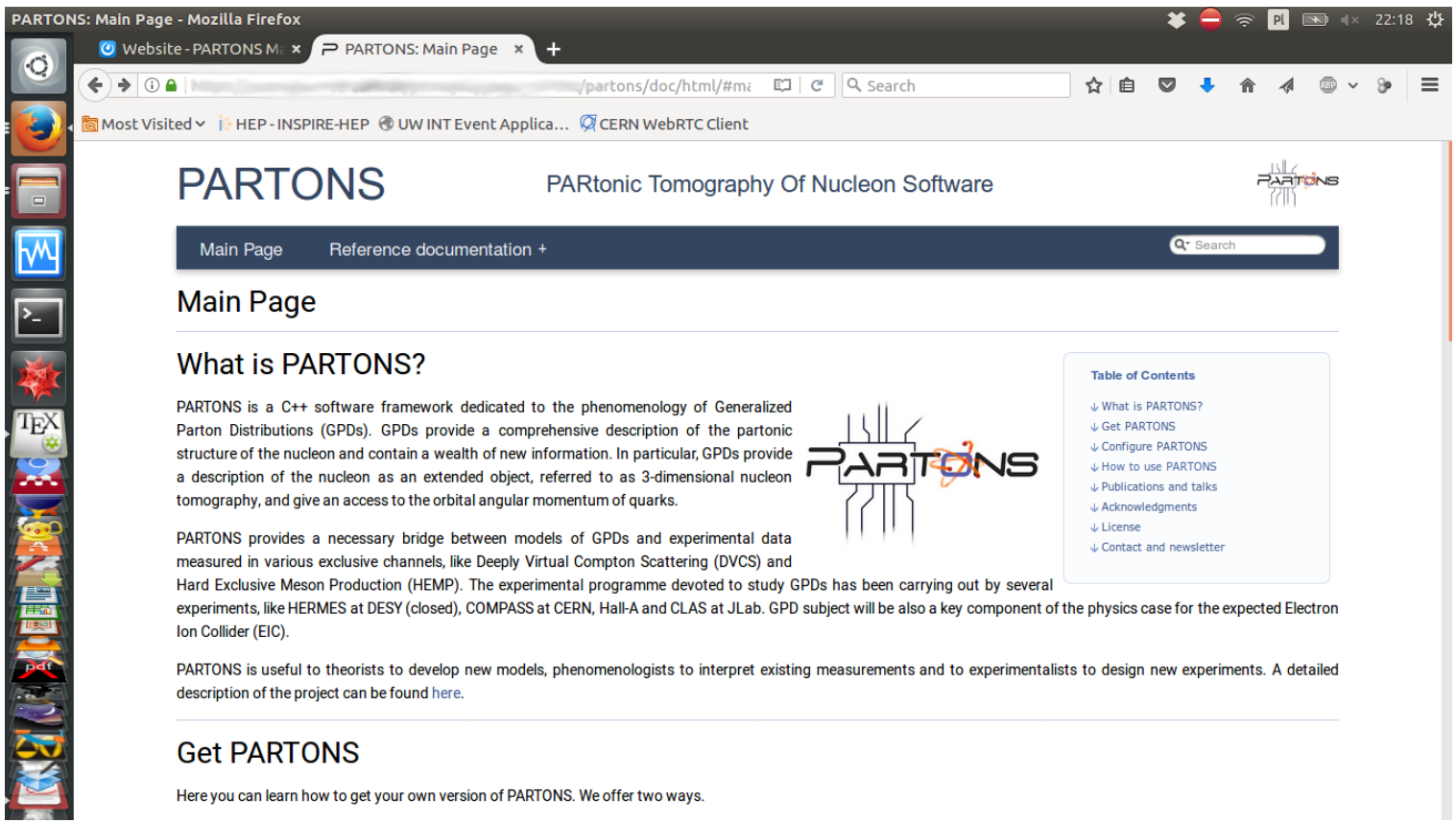

Summary

- GDPs enter factorization theorems for hard exlusive reactions (DVCS, deeply virtual meson production etc.), in a similar manner as PDFs enter factorization theorem for DIS
- First moment of GPDs enter the Ji's sum rule for the angular momentum carried by partons in the nucleon.
- Fourier transform of GPD's to impact parameter space can be interpreted as „tomographic" 3D pictures of nucleon, describing charge distribution in the transverse plane, for a given value of x.
- We are waiting for EIC!